FINAL REPORT
for
A Cooperative Agreement Between
the Flood Control District of
Maricopa County
and the USDA-ARS 4/13/93

FINAL REPORT

A COOPERATIVE AGREEMENT BETWEEN THE FLOOD CONTROL DISTRICT OF MARICOPA COUNTY

AND

THE UNITED STATES DEPARTMENT OF AGRICULTURE AGRICULTURAL RESEARCH SERVICE

FCD - IGA Number 91004
ARS Agreement Number 58-5342-1-129

April 6, 1993

TABLE OF CONTENTS

INTRODUCTION

This document consitutues the final report prepared in accordance with A COOPERATIVE AGREEMENT BETWEEN THE FLOOD CONTROL DISTRICT OF MARICOPA AND THE UNITED STATES DEPARTMENT OF AGRICULTURE, AGRICULTRUAL RESEARCH SERVICE (the Cooperative Agreement).

Several tasks were enumerated within the cooperative agreement. This document is organized by those defined tasks. Each section of this report will state the cooperative agreement task then present any data, analysis, discussions, and conclusions ARS personnel have obtained in accordance with the task. Task numbers correspond to those of the original Scope of Work. Tasks 1-4 consist of background information. Some Tasks from the Scope of Work have been deleted under mutual agreement by the two parties involved.

TASK 5.3: CHECK RAW DATA FROM WALNUT GULCH EXPERIMENTAL WATERSHED, SELECT A SUBSET OF HIGH QUALITY DATA, AND DEVELOP A SET OF RUNOFF DATA OVER A RANGE OF SCALES.

Material collected and transferred to FCDMC in accordance with this task is presented under a separate cover in a report entitled "Documentation for Select Precipitation/Runoff Event Data Sets, Data Sets of Runoff and Associated Precipitation Collected at the USDA - ARS Walnut Gulch Experimental Watershed, Tombstone, Arizona". The separate submittal includes a diskette containing the event data sets, and was deemed necessary for ease of portability.

TASK 5.4 IDENTIFY SUBWATERSHEDS WITHIN THE WALNUT GULCH EXPERIMENTAL WATERSHED WITH A VARIETY OF SOIL COVERS

The USDA-Soil Conservation Service (SCS) is currently working in Walnut Gulch and will begin soil pit work in April. Upon completion of this survey, SCS review of the soil survey, and digitization of the soil boundaries the results will be forwarded to the Maricopa Flood Control District.

TASK 5.5 PERFORM POINT AND PLOT SCALE MEASUREMENTS TO ESTIMATE SOIL SATURATED HYDRAULIC CONDUCTIVITY AND SORPTIVITY USING A DISK PERMEAMETER AND THE RAINFALL SIMULATOR

and

TASK 5.6 USE RAINFALL SIMULATORS AND DEVICES FOR MEASURING SOIL HYDRAULIC PROPERTIES TO MONITOR RAINFALL AND RUNOFF

The CSIRO disk permeameter was used to gather point measurements of soil hydraulic properties. The CSIRO disk permeameter is a column apparatus designed to measure the infiltration of water into field soils at constant and specified heads (tensions.) Based on the research by Perroux and White (1988), the hydraulic conductivity of the soil under saturated and unsaturated conditions can be calculated. Additionally, the macroscopic capillary length and mean pore size of the soil can be calculated from the hydraulic conductivity values.

Disk permeameter data has been collected at two sites within the Walnut Gulch Experimental

Watershed, Tombstone, Arizona. At the Bernadino site, disk permeameter data was collected in November, 1992, April, 1992 and July 1992. The Lucky Hills site was sampled in July 1992. The disk permeameter data set consists of 13 paired samples: at the Bernadino site, four paired samples were taken in November, three in April, and four in July; at Lucky Hills, two paired samples were taken in July, 1992. A paired sample consists of readings from a ponded disk permeameter (supplying water at a constant +10 mm head throughout the sampling), and readings from an unponded disk permeameter (supplying water at about -53 mm head constantly throughout the sampling.)

The disk permeameter data has been collected and analyzed according to the CSIRO disk permeameter instruction manual. Still, much variability is to be expected if, as the literature indicates, soil hydraulic properties are highly variable within a soil type.

Table 1 shows average values calculated for disk permeameter data collected at the Lucky Hills and Bernadino site. Results to date indicate that:

1. Hydraulic conductivity values for the ponded and unponded disk permeameter data are significantly different. This is to be expected.

2. No significant temporal differences appear to exist between hydraulic conductivity values gathered at different times of the year.

3. Unsaturated hydraulic conductivity values derived from the disk permeameter seem to correlate better with other hydraulic conductivity data collected at Walnut Gulch than do satruated hydraulic conductivity values.

Table 1. Summary of Point Measurements of Soil Hydraulic Properties

Part A - Lucky Hills Data (Average Values)

Instrument	Steady state infiltration (in/hr)	Sorptivity (in/hr$^{1/2}$)	Hydraulic Conductivity (in/hr)
Unsaturated permeameter (head = - 2.2 in)	0.47	0.44	0.32
Satruated permeameter (head = + 0.3 in)	3.63	1.18	2.90

Part B - Bernadino Simulator Site Data (Average Values)

Instrument	Steady state infiltration (in/hr)	Sorptivity (in/hr$^{1/2}$)	Hydraulic Conductivity (in/hr)
Unsaturated permeameter (head = - 2.2 in)			
July, 1992	0.49	0.42	0.35
April, 1992	0.83	0.74	0.36
November, 1991	0.53	0.54	0.36
Saturated permeameter (head = + 0.3 in)			
July, 1992	6.11	1.55	4.00
April, 1992	5.04	1.57	3.43
November, 1991	10.03	2.62	5.36

In terms of scaling hydraulic conductivity estimates from point to plot to small watersheds a relatively consistent set of estimates appears to be emerging. In the Lucky Hills subwatersheds region of Walnut Gulch soil hydraulic conductivity estimates are now available from the disk permeameter, rainfall simulator plots and as estimated from a research version of a calibrated and verified distributed rainfall-runoff model (KINEROS) (Woolhiser et al., 1990) on three small, nested, subwatersheds. The disk permeameter measurements are from the unponded, or tension, disk permeameter (supplying water at either -52 or -54 mm constantly throughout the sampling) measurements. The simulator plot estimates are obtained from very wet runs on natural cover condition plots. The distributed rainfall-runoff model estimates were based on the Smith-Parlange (1978) infiltration model incorporated within KINEROS. Very good model estimates were obtained from the model for each of the three subwatersheds as judged by the Nash-Sutcliffe forecast coefficient of efficiency on runoff volume (E_V) and peak runoff rate (E_Q) (Nash and Sutcliffe, 1970). The coefficient of efficiency was selected because it is dimensionless and is easily interpreted. If the model predicts observed runoff volume or peak runoff rate with perfection, E_V and E_Q both equal one (1). If $E < 0$, the model's predictive power is worse than simply using the average of observed values. The efficiency statistics and standard statistics for the three watersheds are summarized in Tables 2 and 3. In addition, internal, distributed model consistency was also achieved by checking internal model results on the two nested subwatersheds internal to LH-104, namely LH-106 and LH-102.

These results demonstrate that the model was effective for independent event prediction. Given these results some confidence can be associated with the saturated hydraulic conductivity estimates inferred from the model. For a more complete description of the model calibration and validation methodology see Appendix 2, which is chapter 5 from Goodrich (1991).

Table 4 summarizes the steady state infiltration parameters derived from the three methods for the Lucky Hills soils. Results from Table 4 indicate that it may be possible to scale point and runoff plot estimates to the small watershed scale.

Table 2. Calibration and Verification Forecasting and Prediction Efficiencies for Runoff Volume and Peak Rate for All Study Basins

		Calibration Efficiencies				Verification Efficiencies			
		E_f		E_p		E_f		E_p	
Basin	Area (ac)	V	Qp	V	Qp	V	Qp	V	Qp
LH-106 $n_c = 10$ $n_v = 17$	0.89	0.98	0.95	0.98	0.98	0.98	0.79	0.98	0.83
LH-102 $n_c = 10$ $n_v = 17$	3.46	0.97	0.97	0.97	0.97	0.93	0.93	0.94	0.95
LH-104 $n_c = 9$ $n_v = 16$	10.9	0.97	0.98	0.97	0.98	0.99	0.96	0.99	0.97

n_c = number of calibration events
n_v = number of verification events

Table 3. Mean and Standard Deviation for Volume and Peak Rates and Average Sum of Squared Deviations for Calibration and Verification Event Sets for All Study Basins

Basin	Area (ac)	Event Set	Type	Num. of Events	V (mm) Mean	V (mm) S.D.	Qp(mm/hr) Mean	Qp(mm/hr) S.D.	Average Sum of Sq. Dev. $(mm/hr)^2$
LH-102	0.89	Calib.	Obs.	10	4.74	5.03	34.2	36.8	
			Sim.	10	4.78	4.98	35.6	36.8	520
		Verif.	Obs.	17	6.22	11.4	27.1	36.7	
			Sim.	17	6.96	12.1	33.3	38.5	1170
LH-102	3.46	Calib.	Obs.	10	4.57	4.48	27.6	27.8	
			Sim.	10	4.36	4.61	26.5	27.7	258
		Verif.	Obs.	17	6.01	9.88	24.6	26.6	
			Sim.	17	6.76	12.1	25.3	31.1	688
LH-104	10.9	Calib.	Obs.	9	4.27	4.49	28.0	30.1	
			Sim.	9	4.44	4.99	24.8	29.3	343
		Verif.	Obs.	16	6.37	11.9	26.3	34.6	
			Sim.	16	6.76	12.3	23.0	30.2	897

Table 4. Steady State Infiltration Estimates for the Lucky Hills Soils from Three Different Methods

Method	Area	Steady State Infilt. Estimate (in/hr)
Unponded Disk Permeameter[1]	0.36 ft^2	0.32
Rainfall Simulator[2]	377 ft^2	0.32
KINEROS R-R Model[3]		
LH-106	0.89 ac	0.43
LH-102	3.46 ac	0.39
LH-104	10.9 ac	0.43

[1] Average of 2 measurements
[2] Average of 2 simulator runs
[3] Estimates are based on area weighted averages of distributed model elements.

TASK 5.7: COLLECT NEW DATA AND ANALYZE EXISTING DATA TO PROVIDE A REASONABLE DESCRIPTION OF LOSSES RESULTING FROM SHEET FLOW AS WELL AS CHANNEL TRANSMISSION LOSSES

The three Lucky Hills watersheds described in task 5.6 (LH-106, 0.89 ac; LH-102, 3.46 ac; LH-104 10.9 ac) provide a good estimate of loss rates that may be expected from sheet flow. These small watersheds are located in upland areas with a small channel system that comprises less then five percent of the basin area for each of the three catchments. The channel system is quite small and on typical USGS 1:24,000 maps these small catchments would have no channel system as represented by a map blueline and would be treated as hillslope areas. At the Lucky Hills watershed scale, channels with coarse alluvium have not developed and therefore channel losses at this scale are not important. The Smith-Parlange (1978) loss rate parameters for each of the three watersheds are presented in Table 5. These estimates are based on application of the KINEROS model to these watersheds discussed in task 5.6 and Appendix 1.

Table 5. Smith-Parlange (1978) Infiltration Parameter Estimates and Vol. Rock Content used in the Application of KINEROS to the Lucky Hills 106, 102 and 104 catchments.

Catchment	Area	Sat. Hydr. Cond. (in/hr)[1,2]	Effective Net Cap. Drive (in)[1,3]	Volumetric Rock Cont.[1,4]
LH-106	0.89 ac	0.43	10.44	0.388
LH-102	3.46 ac	0.39	9.60	0.372
LH-104	10.9 ac	0.43	9.02	0.388

[1] Estimates are based on area weighted averages from multiple distributed model elements.
[2] Parameter "FMIN" in KINEROS
[3] Parameter "G" in KINEROS
[4] Parameter "ROC" in KINEROS

Loss rates for channel transmission are discussed more fully in the following task section (5.8)

TASK 5.8: DEVELOP LOSS PARAMETERS THAT CAN BE USED TO CALIBRATE ROUTING OF FLOOD WAVES THROUGH A CHANNEL

Channel loss analysis for relatively incised channels from Walnut Gulch flumes above flume 6 to flume 6 has been completed for several well checked events. Events were selected to isolate storm cells such that lateral inflow between the flumes would not exist and would not complicate estimation of channel losses. For the selected events, associated total rainfall isoline plots are presented in Appendix 3. The geometry of channel segments used in the analysis is described by Unkrich and Osborn (1987, included in Appendix 2) and is summarized in Appendix 3. A primary conclusion of Unkrich and Osborn (1987) was that widely variable steady state channel infiltration rates would be necessary for the model to accurately predict observed flow. Since the study of Unkrich and Osborn (1987) a variable wetted perimeter algorithm has been incorporated in the channel infiltration and routing portions of KINEROS (Woolhiser et al., 1990; see page 25 for more detail, and the last figure of Appendix 3).

For the selected events, channel loss parameters were estimated directly, without calibration to observed runoff data, based upon soil textrual class (see Woolhiser et al., 1990, pages 8-9). For the coarse, sandy channels typical of Walnut Gulch the saturated hydraulic conductivity ("FMIN" in KINEROS) estimate is 8.3 in/hr. This parameter and the associated suction parameter of G = 1.8 inches (net effective capillary drive) were used in the model without calibration. Using these parameters the variable wetted perimeter routing and infiltrating method was compared to the prior method used by Unkrich and Osborn (1987) in which infiltration is assumed to occur over the entire trapezoidal wetted perimeter.

Table 6 summarizes the results for the two models and four of the events are plotted in Figure 1. In these figures time adjustments to match the peak have been made to enable more ready comparison. Adjustments are justified on a physical basis as independent mechanical clocks are at each flume and a +/- 10 minute error in timing is not uncommon. It is apparent that the new variable wetted perimeter method does much better for both peak runoff rate estimation and for runoff volume as the recessions more closely match the observed data. These represent very good results for uncalibrated model application. Some parameter adjustment might improve the results but the type of observed data required to make these estimates is rarely available outside the USDA-ARS Walnut Gulch Experimental Watershed.

Table 6. Observed versus Full and Variable Wetted Perimeter Model Results

Date	Peak Rate (cfs) Obs.	Peak Rate (cfs) Full	Peak Rate (cfs) Var.	Volume (ac-ft) Obs.	Volume (ac-ft) Full	Volume (ac-ft) Var.
18 Aug 74	947	895	911	48.8	41.5	51.4
22 Jul 75	702	635	662	39.7	28.2	44.4
22 Aug 75	317	226	263	8.08	4.95	9.09
28 Jul 76	346	234	305	23.2	10.7	22.6
10 Aug 76	560	520	555	33.4	19.4	33.02

14

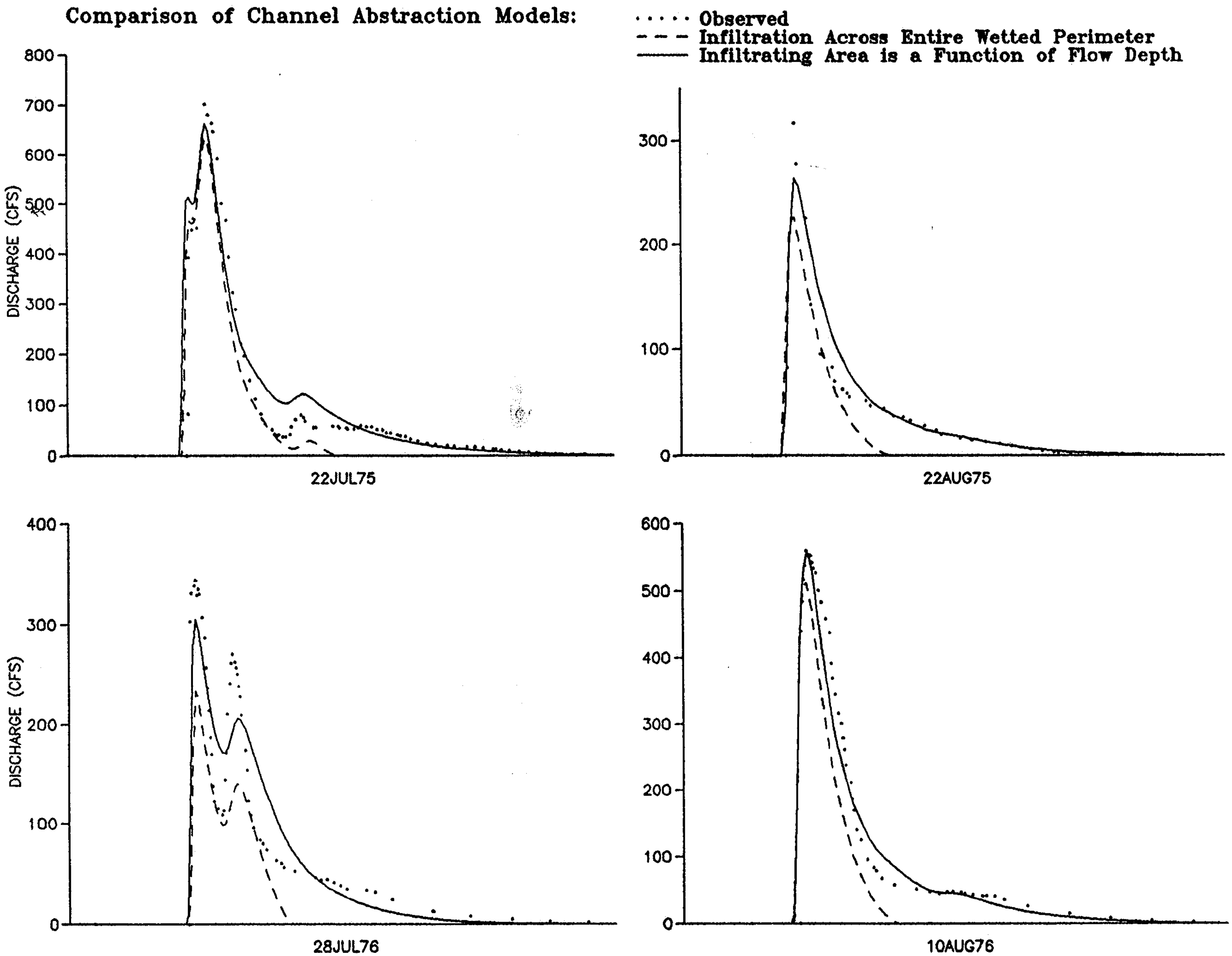

Comparison of Channel Abstraction Models:
Observed
Infiltration Across Entire Wetted Perimeter
Infiltrating Area is a Function of Flow Depth
DISCHARGE (CFS)
800
700
600
500
400
300
200
100
0
22JUL75
300
200
100
0
22AUG75
DISCHARGE (CFS)
400
300
200
100
0
28JUL76
600
500
400
300
200
100
0
10AUG76

Figure 1

TASK 5.12: SUBMIT QUARTERLY PROGRESS REPORTS TO THE DISTRICT

Three previous quaterly reports in accordance with this agreement have been delivered.

TASK 5.14: PROVIDE A FINAL REPORT OF RESEARCH RESULTS UPON COMPLETION OF THE PROJECT. ALL RELEVANT FIELD DATA AND MAPS, INCLUDING SOIL AND VEGETATION, AND WATERSHED DELINEATIONS WILL BE DELIVERED WITH THE FINAL REPORT

This document consitutes the final report.
All digital data is provided on a 3½-inch high density diskette

TASK 5.14.1 Provide a set of Walnut Gulch Orthophoto Maps with contours.
TASK 5.14.2 Provide a set of Walnut Gulch Orthophoto Maps without contours.

Figure 2 shows the 1:5000 - scale map boundaries superimposed over the outline of the watershed.

This set of maps was previouly delivered to Mr Steve Waters, the Maricopa Flood Control project manager. Since that delivery the maps are undergoing some minor revisions on subbasin boundary locations and at map sheet boundaries. The necessary revisions have been made in a temporary (non-inked) fashion on the orthophotos. However the revisions have been incorporated into the GIS-compatible boundary files. Once permanent revisions are made to the maps a new sets of reproductions will be forwarded to the Maricopa Flood Control District.

The files containing the watershed and subwatershed boundary coordinates are contained in files on the 3½-inch diskette submitted with this report. These coordinates are based on a NAD 1927 datum consistent with the orthophoto maps discussed above. The vegetation boundaries were obtained from a planimetric map of the watershed dated 1952. This vegetation survey nor the map it was placed on is of consistent accuracy with the 1:5000 orthophoto maps mentioned above. Figure 3 shows the vegetation produced from the digitized vegetation data.

Walnut Gulch Subwatershed and 1:5000 Map Boundaries

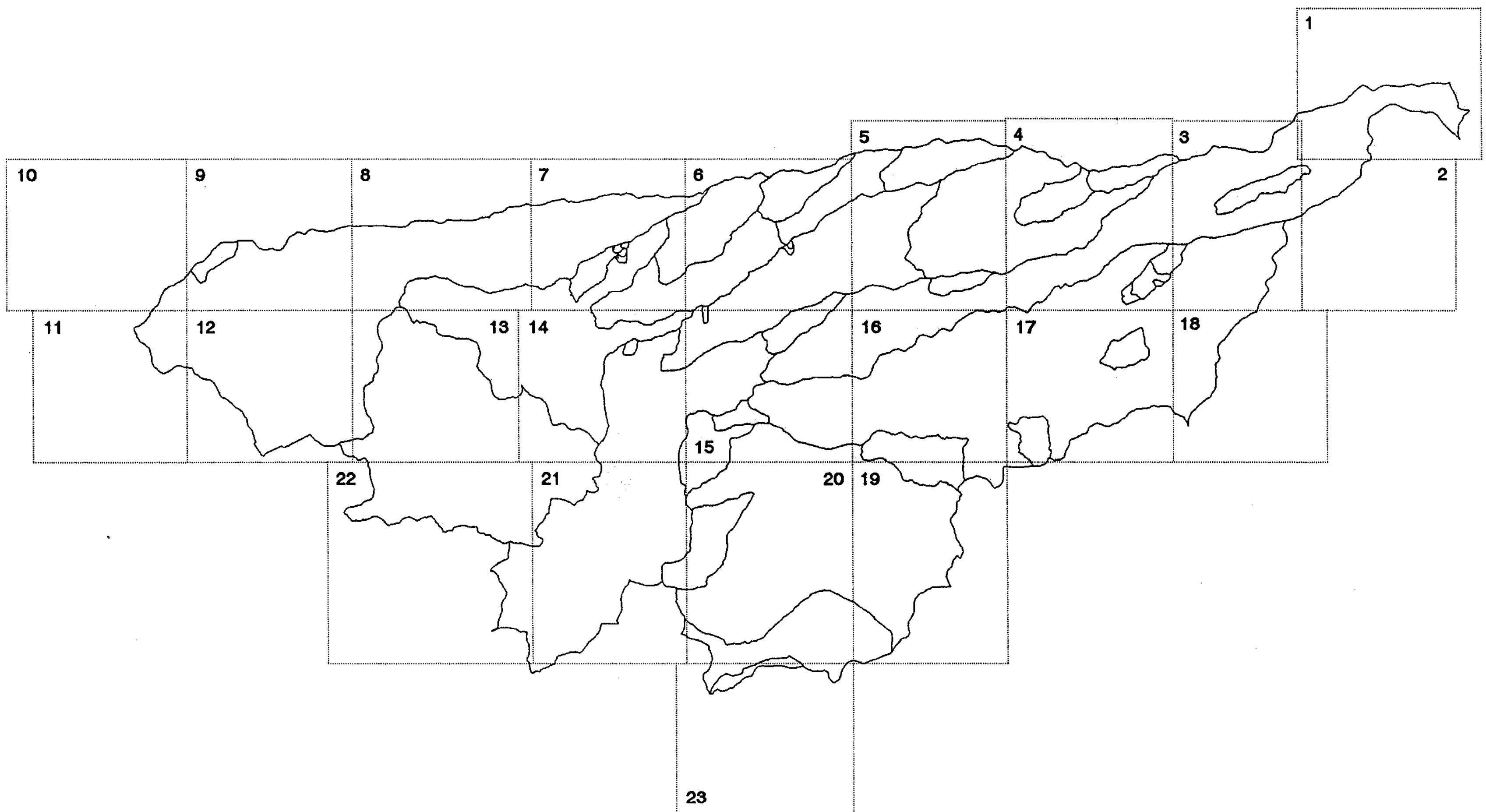

Figure 2

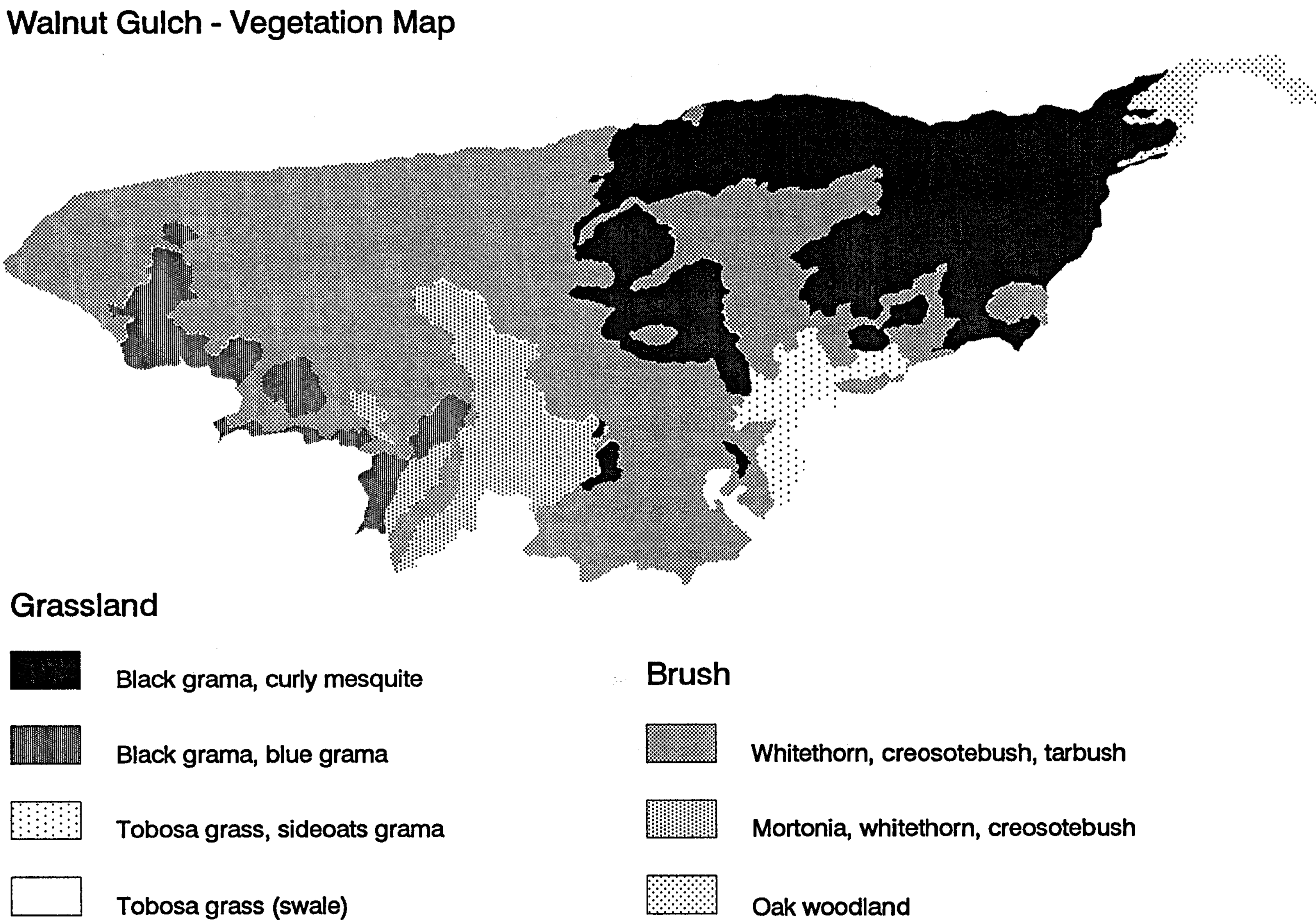
Walnut Gulch - Vegetation Map
Grassland
Black grama, curly mesquite
Black grama, blue grama
Tobosa grass, sideoats grama
Tobosa grass (swale)
Brush
Whitethorn, creosotebush, tarbush
Mortonia, whitethorn, creosotebush
Oak woodland

Figure 3

References

Goodrich, D. C., Basin scale and runoff model complexity. Univ. of Arizona, Dept. of Hydrology and Water Resour. Tech. Rep. No. HWR 91-010, 361 p., June, 1991.

Nash, J. E., and J. V. Sutcliffe, 1970. River flow forecasting through conceptual models, I. A discussion of principles. Journal of Hydrology, 10:282-290.

Perroux, K. M., and I. White, 1988. Designs for disk permeameters. Soil Sci. Soc. Am. J., 52:1205-1215.

Smith, R. E., and Parlange J.-Y., 1978. A parameter-efficient hydrologic infiltration model. Water Resources Research, 14(33):533-538.

Unkrich, C. L., and H. B. Osborn, 1987. Apparent abstraction rates in ephemeral channels. Hydrology and water resources in Arizona and the Southwest. Proc. 1987 Am Water Resour. Assoc., Ariz.-Nev. Acad. of Sci. and Ariz. Hydrol. Soc., [Flagstaff, Ariz., April 1987]. Vol. 17, p. 35-42.

Woolhiser, D.A., Smith, R.E. and Goodrich, D.C., 1990. KINEROS, A Kinematic Runoff and Erosion Model: Documentation and User Manual. U.S. Dept. of Agriculture, Agricultural Research Service. ARS-77. 130p.

FINAL BUDGET REPORT

Project Expenditures:

	ITEM	AMOUNT
1.	ARS Project Overhead (10%)	$ 3,000.00
2.	Wages and benefits for 20 two week pay periods at $934.41/pay period (thru Dec. 31)	18,688.20
3.	Two days travel per diem to Tombstone, AZ	30.00
4.	Office chair	200.04
5.	Office Supplies	41.67
6.	Computer Supplies	81.20
7.	Axum Graphics Software	305.00
8.	GBSTAT Statistics Software	259.95
9.	UA Fastcopy - Journal Article	6.17
10.	USGS-WRI Report 83-4159	8.75
11.	Silicone Sealant	3.06
12.	Disk Peameameter Supplies	32.48
13.	Blueline Copies of Walnut Gulch Maps	69.62
14.	Stiffener material	1.06
15.	Plastic Bags	2.02
16.	Nylon Membrane	29.40
17.	Soil Crusting: Text	90.00
18.	Line Printer Contribution	203.28
19.	Norton Utilities and Editor	106.05
20.	Sand and electrical tape for disk Perm.	11.85
21.	Franklin Project Planner	100.87
22.	Wages and benefits for 6 two week pay periods at $976.46/pay period (cost of living adjustment to 2/13/93)	$ 5,858.76
23.	Tombstone per Diem	30.00
24.	Windows 3.2	115.45
25.	Wordperfect for Windows	141.75
26.	387 Math CoProcessor	94.05
27.	GB-STAT software update	94.95
28.	Lump Sum for unused annual leave (Doolen)	287.78

TOTAL EXPENSES $ 29,893.41

BALANCE **$ 30,000.00 - 29,893.41 =** **$ 106.59**

APPENDIX 1

"Basin Scale and Runoff Model Complexity" - excerpt

CHAPTER 5

MODEL SENSITIVITY, CALIBRATION, AND VERIFICATION

5.1 Introduction and Background

The geometric model simplification procedures introduced in the last chapter were tested on a small watershed, the parameters of which were estimated from field measures. A reasonable level of confidence exists in the definition of geometric (topographic) parameters given the availability of large-scale maps and the ability to directly measure channel geometries. A much lower degree of confidence exists in the hydraulic roughness and soil hydraulic parameter estimates as they were not directly measured nor can they be easily measured. Therefore, model calibration to better estimate these highly uncertain parameters is required.

To acquire greater confidence in the model, the simplification procedure and subsequent interpretations regarding basin dynamics, verification, in addition to calibration, with observed data is required. Without verification using observed data, study conclusions must be confined to the realm of the computer and its simulations. If model confidence can be acquired with rainfall-runoff data, a degree of realism can be attached to the conclusions of this study and valid insights into actual watershed process behavior can be obtained. Beven (1989) pointed out that great care must taken in making interpretations regarding distributed hydrologic model predictions. The primary objective of this chapter is to demonstrate model realism and to ensure that realistic interpretations can be made.

Calibration and verification of distributed rainfall-runoff models are made difficult by the very nature of distributed systems. Beck (1987) noted that the intrinsic problem due to aggregation is that the dimension of the input/output observations is much smaller than those of the state and parameter vectors. Aggregation, as implied by Beck, denotes the discretization of space-time domain. Because partial differential problem formulations are by nature, continuous, we cannot track all states and parameters over the entire space-time domain and, therefore, must aggregate to make the problem tractable. Verification of distributed states and parameter vectors would require an observation system so elaborate that it is infeasible. Without adequate data (internal and input/output), identification, and estimation problems result routinely.

The curse of inadequate distributed field data for model calibration and verification was also pointed out by Beven (1988, 1989) and Klemes (1988). Beven concluded that, for modeling continuous flow, more than four or five parameters will result in identifiability problems (Kirkby, 1976; Blackie and Eeles, 1985). More parameters might be allowed with increased field measures of distributed state variables, but such data are rarely available. Warwick (1989) concurred with this conclusion noting that increases in process model complexity will not decrease modeling error unless data sampling is increased. Therefore, due to the paucity of distributed data, only several parameters should be used for model calibration. Parameter estimation problems introduced by overparameterization and poor model structure are well documented (Sorooshian and Gupta, 1983, 1985; Johnston and Pilgrim, 1976; Jun, 1989).

Beck (1987) equated the lack of parameter identifiability and overparameterization to surplus model content. The crux of the problem is that one would like to know the internal description of a system which is of substantially higher order than what can be observed about the external system description. "The model may contain descriptions either of a type of behavior not actually observed in a sample of data or of multiple types of behavior, the individual components of which cannot be disentangled from observation of their collective effect. The consequences are usually apparent in the absence of a uniquely "best" combination of parameter values that fit the data and result in parameter estimates with high error variances and covariances." (Beck, 1987). Beck also concluded that reducing the number of parameters is equivalent to increasing the number of observed data, and that throwing out the most insensitive parameters is equivalent to discarding the most uncertain parameters.

The primary type of data that will be used to calibrate and verify KINEROSR and the simplification procedure is rainfall-runoff data from the USDA-ARS Walnut Gulch Experimental Watershed. Because these are input/output data, the preceding comments are applicable. However, using the nested Lucky Hills watersheds, some degree of interior model knowledge or confidence can be acquired. The nested basins will allow internal verification of the model. Still, only two internal measures of runoff data are collected within LH-104. Given this constraint, only a small number of "free" optimization parameters are justified in light of the comments above. Sensitivity of dependent model variables (runoff) to parameter variation offers a method to select those parameters which should be included in model calibration.

5.2 Sensitivity to Selected Optimization Parameters

Because the model will be applied, calibrated, and verified over a wide range of events, the sensitivity analysis of runoff to model parameters will also be conducted over a range of runoff event sizes. To conduct the initial sensitivity analysis, the most complex representation of LH-106 (30 elements) as shown in Figure 4.2 was used. Ten runoff events, covering a range of runoff size and initial conditions, were selected from a set of 30, carefully checked, rainfall-runoff events. Geometric model parameters of plane area, slope, and width were measured on 1:480 scale maps with a 1 foot (0.3048 m) contour interval. Channel geometries were measured in the field. Soil samples were taken at six field locations and were used to estimate rock content and soil hydraulic parameters. A more detailed explanation of the estimation of initial model parameters and runoff event selection is presented in Appendix A. Initial soil moisture estimates were computed by the daily water balance component of CREAMS (Knisel, 1980) independently of KINEROSR. Appendix B contains a more detailed summary of the use of CREAMS.

To ensure that initial parameter estimates provided reasonable runoff estimates, a single event (#53) was selected for model fitting. The size of this event falls in the middle of the ten selected events, and it is double peaked, providing a more complex test of the model. The roughness and Ks parameters were selected for initial model fitting after discussions with an experienced KINEROSR user (Woolhiser, personal communication, 1988). User experience indicated that these parameters have significant impact on runoff predictions. Adjustments to these two parameters were made by applying a uniform multiplier to the Ks and roughness of each plane and channel model element over the entire watershed. By doing so, relative differences in field parameter estimates are maintained but are scaled in a linear fashion.

Using the observed rainfall from raingage 83, the roughness and Ks multiplers (parameters) were manually adjusted to fit observed runoff. The simulated and observed hydrograph for event 53 for the best set of multipliers is presented in Figure 5.1. The simulated runoff volume, peak runoff rate, and time to peak agree to within 0.15 percent of the respective observed data.

Beven (1989) noted that it is very easy to fit a single rainfall-runoff event. The fitting exercise above proves this and is not meant to serve as a general endorsement of KINEROSR. The exercise of obtaining the manually derived parameter multipliers is only meant to start, or center, the sensitivity analysis around a range of values which will produce reasonably realistic runoff simulations for all ten events. Table A.1 in Appendix A provides observed summary runoff information for these ten events (highlighted by an asterisk in table A.1).

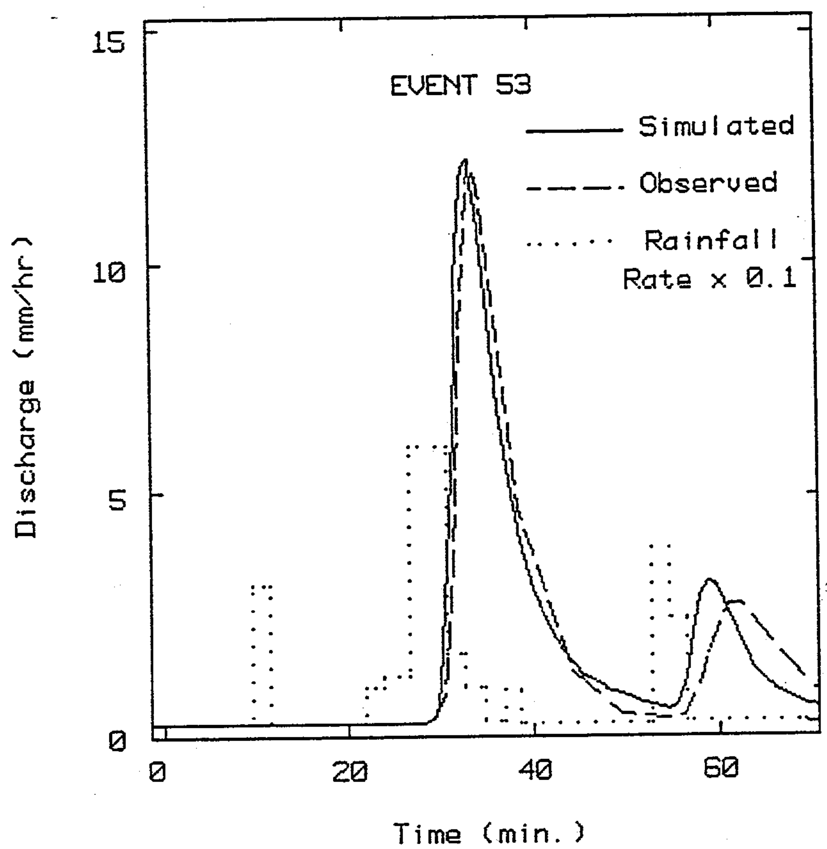

Figure 5.1 Observed Versus Simulated Runoff for Event 53 (Roughness and Ks Parameter Multipliers Manually Adjusted)

Runoff volume, peak runoff rate, and time to peak will be used to assess the sensitivity of runoff characteristics to changes in various parameters. Univariate sensitivity analysis is carried out using the uniform multiplier approach described above. Model sensitivity due to multiple parameter interactions is indirectly addressed later in this chapter when optimization results are discussed. Table 5.1 contains a list of the parameters considered in the sensitivity analysis and a brief description of how they are used in the model.

The parameters selected for the sensitivity analysis are those that cannot be measured directly in the field with a high degree of confidence. Parameters that can be directly and accurately measured are excluded from the analysis. Field measured values for these parameters will be input into the model. It is assumed that they can be determined with sufficient accuracy so that very little uncertainty is introduced into simulated runoff by the uncertainty in these parameters. Also excluded are those parameters which can be determined by repeatable, objective, rules, such as characteristic computational length (CLEN) discussed in the previous chapter.

Uniform multipliers of 0.9 and 1.1, corresponding to a +/- 10% parameter perturbation, were applied to all of the parameters listed in Table 5.1. The roughness and Ks parameters for planes and channels were considered independently to see if some insight into the relative domination of channel or overland flow processes could be acquired. The results are presented graphically in Figure 5.2 to illustrate the effect of the parameter perturbations over the full range of the ten selected events. The effects on the time to peak (Tp), peak runoff rate (Qp), and

Table 5.1. KINEROSR Model Parameters Used in the Sensitivity Analysis

Parameter	Units	Description
C_v	---	Coefficient of variation of Ks
DINTR	L	Interception depth
Ks_p	L/T	Saturated hydraulic conductivity for overland flow planes. Note: If obtained for soil it should be corrected for volume of rock.
Ks_c	L/T	Saturated hydraulic conductivity for channels
POR	---	Soil porosity
$R1_p$	---	Manning's n for overland flow planes
$R1_c$	---	Manning's n channels
RECS	---	Infiltration recession factor
ROC	---	Volumetric rock content of soil
SI	---	Initial relative soil saturation
SMAX	---	Maximum relative saturation under imbibition

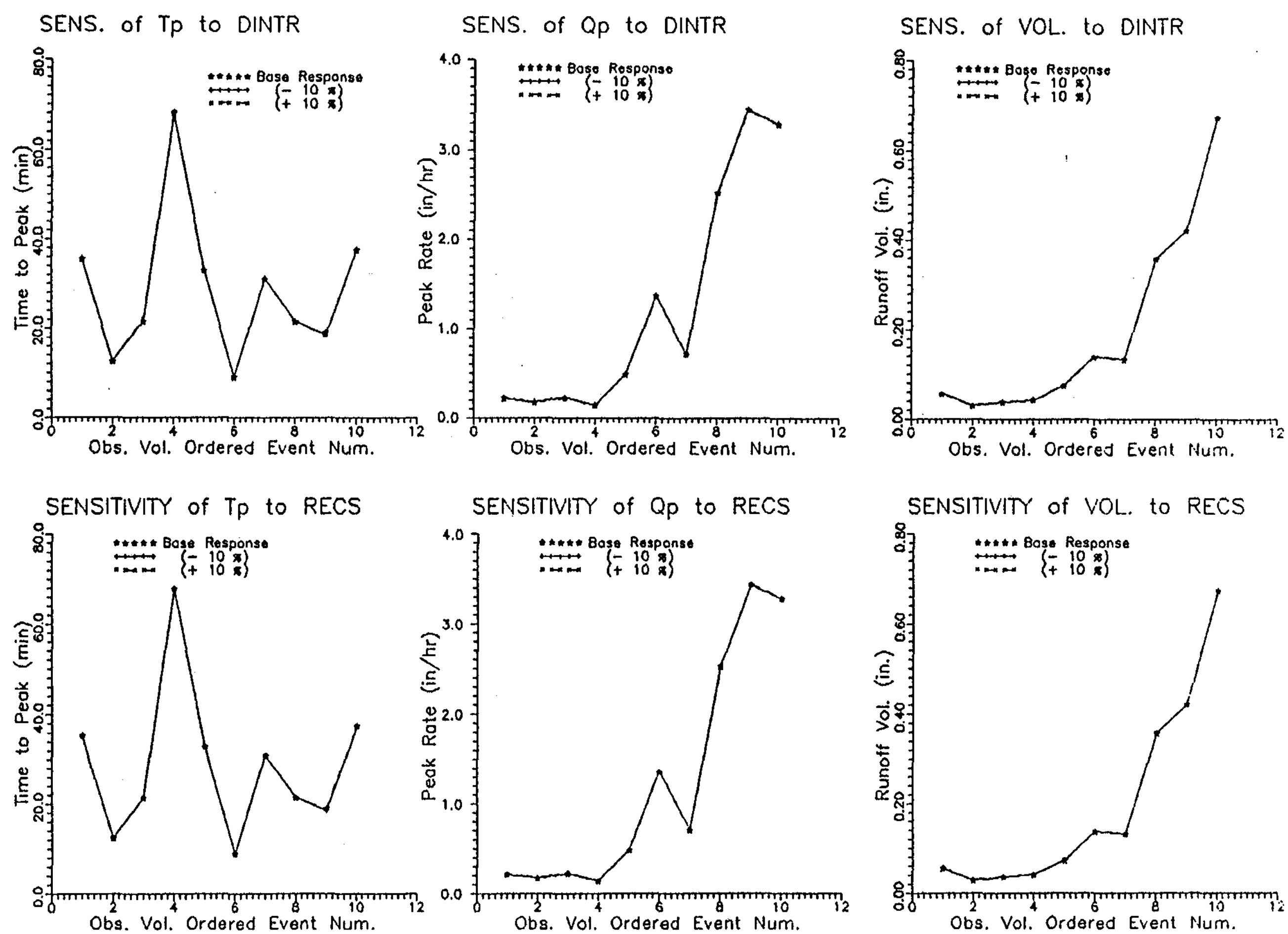

Figure 5.2 Sensitivity of Tp, Qp, and VOL. of Simulated Runoff to a -/+ 10% Perturbation of Selected Model Parameters Over a Range of Ten Events

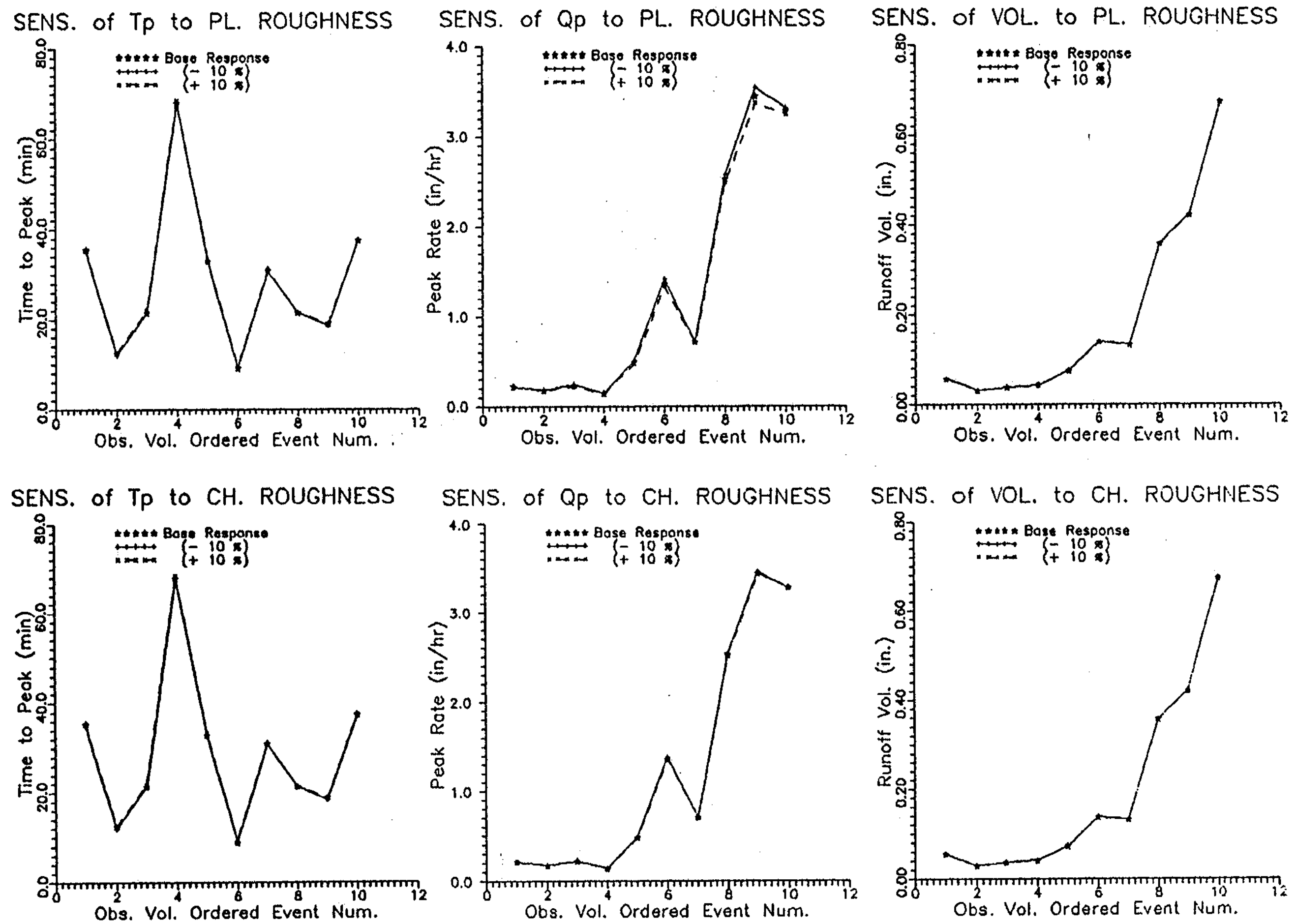

Figure 5.2 Sensitivity of Tp, Qp, and VOL. of Simulated Runoff to a -/+ 10% Perturbation of Selected Model Parameters Over a Range of Ten Events - (Continued)

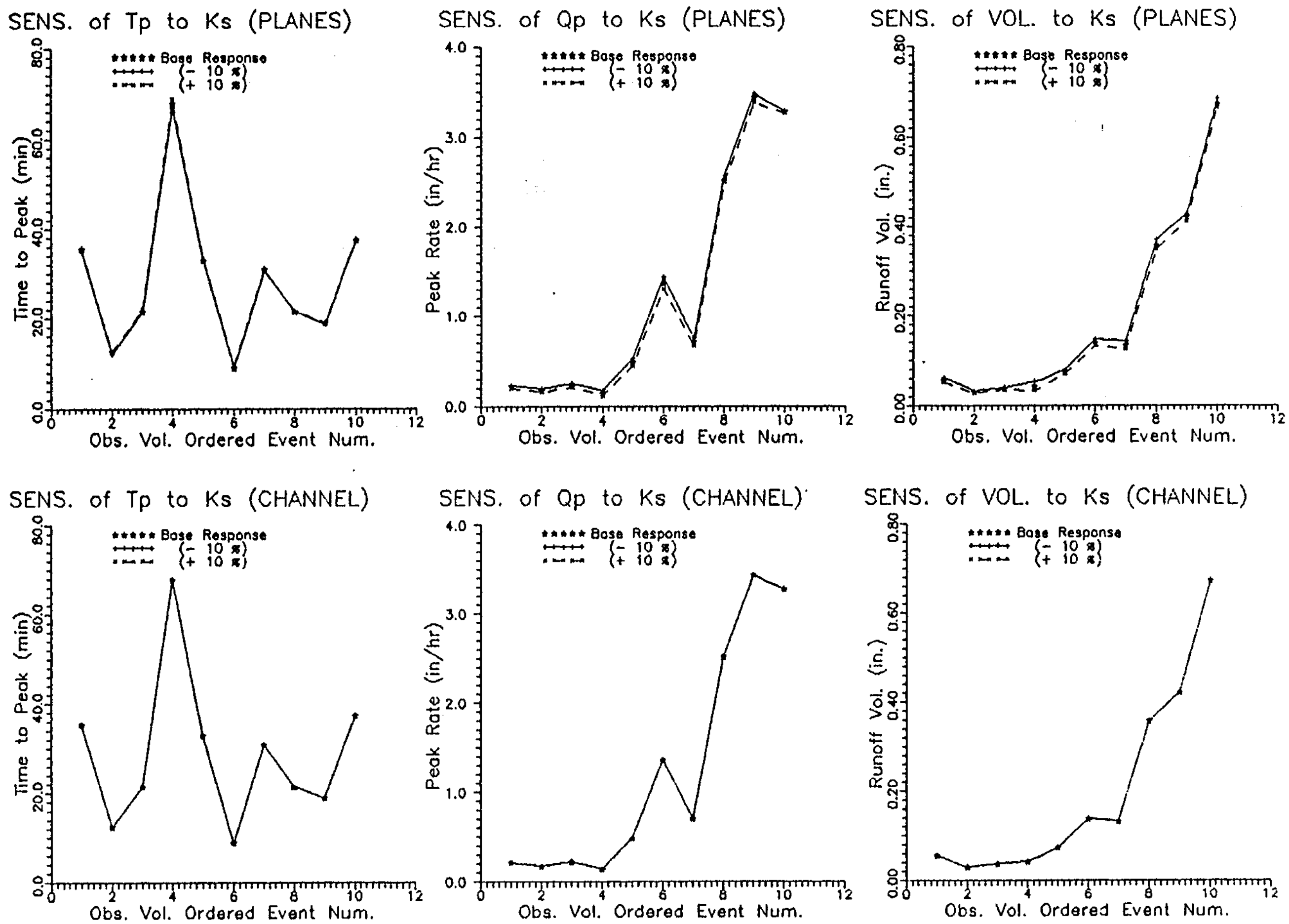

Figure 5.2 Sensitivity of Tp, Qp, and VOL. of Simulated Runoff to a -/+ 10% Perturbation of Selected Model Parameters Over a Range of Ten Events - (Continued)

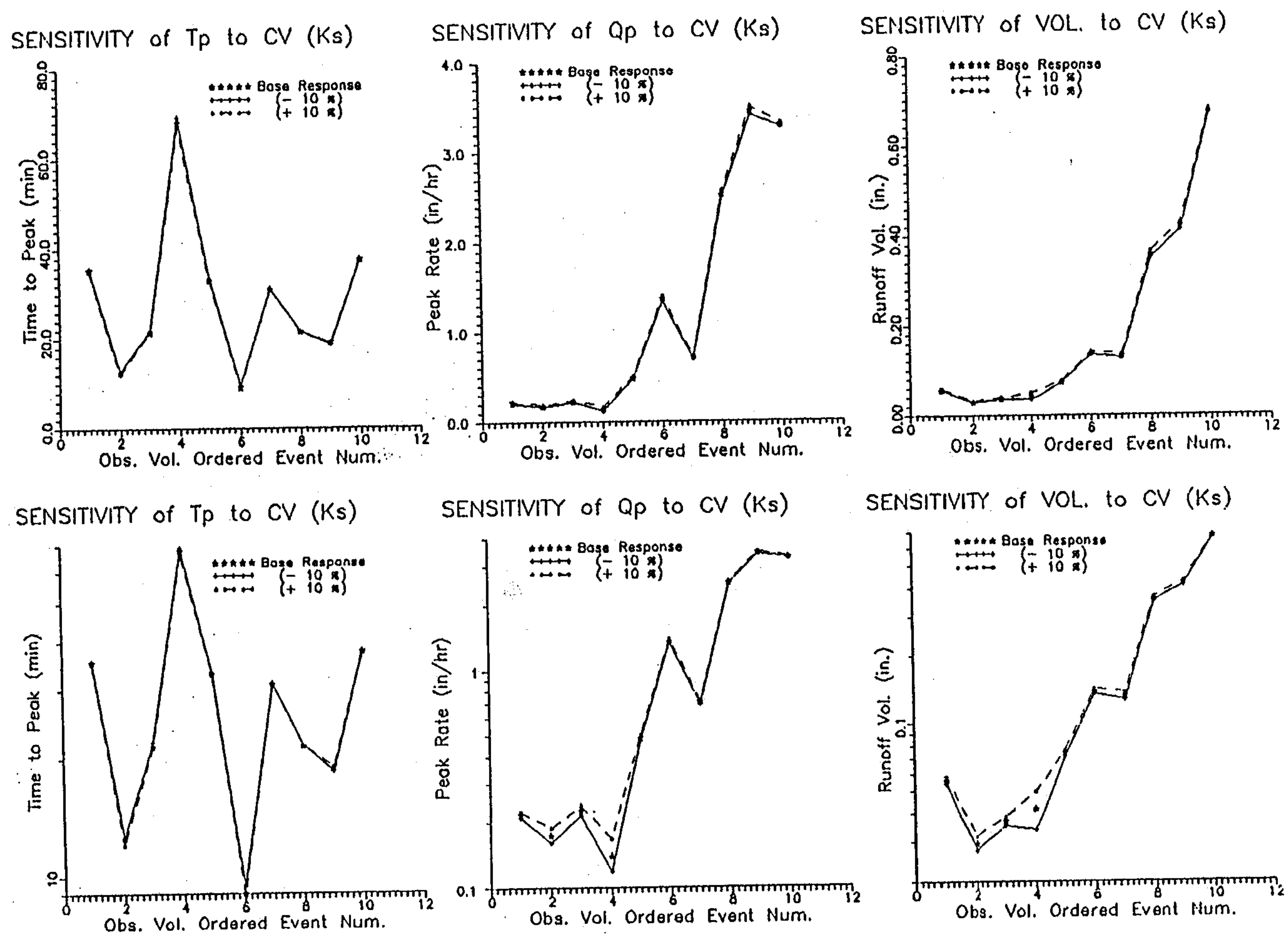

Figure 5.2 Sensitivity of Tp, Qp, and VOL. of Simulated Runoff to a -/+ 10% Perturbation of Selected Model Parameters Over a Range of Ten Events - (Continued)

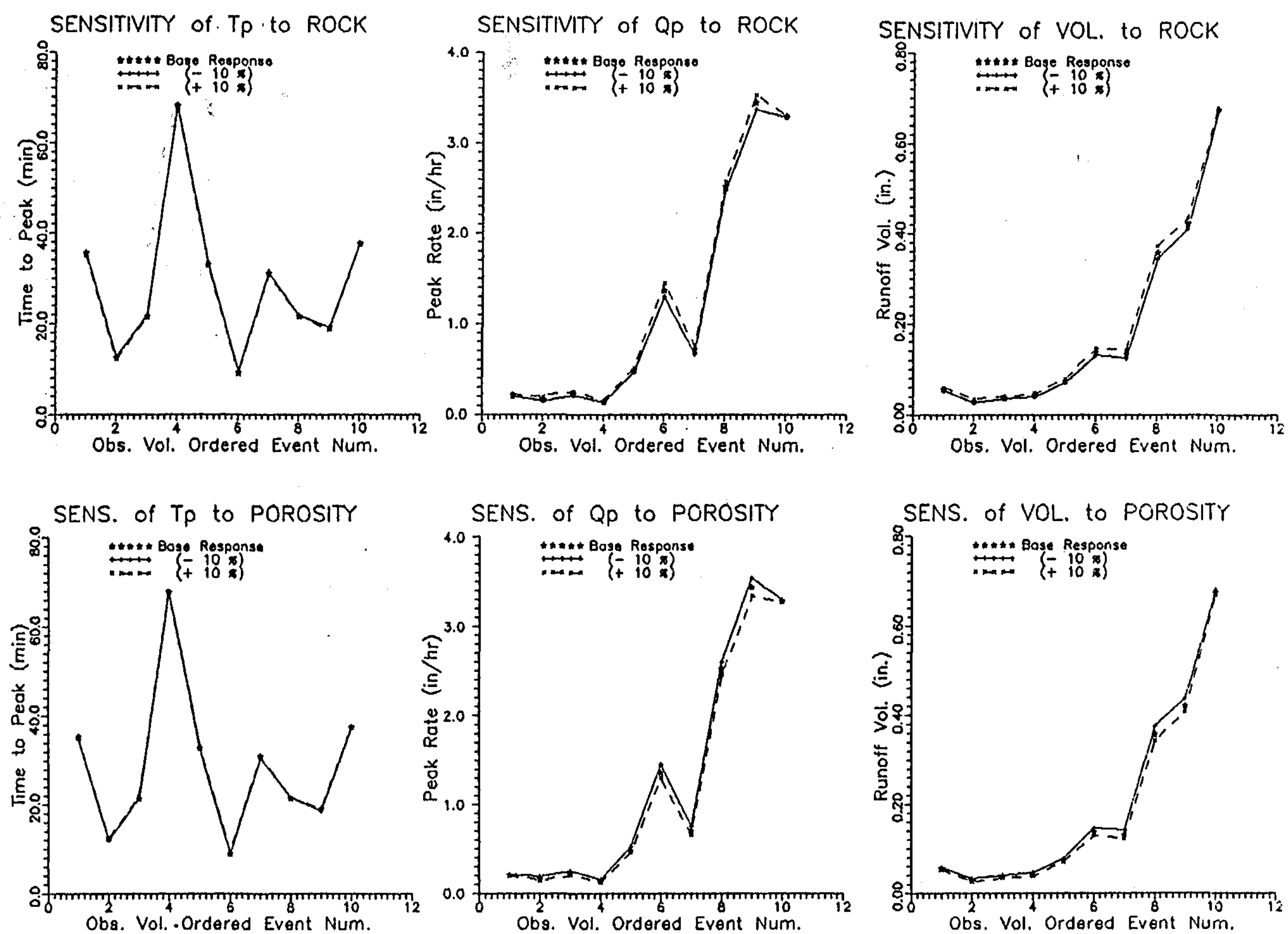

Figure 5.2 Sensitivity of Tp, Qp, and VOL. of Simulated Runoff to a -/+ 10% Perturbation of Selected Model Parameters Over a Range of Ten Events - (Continued)

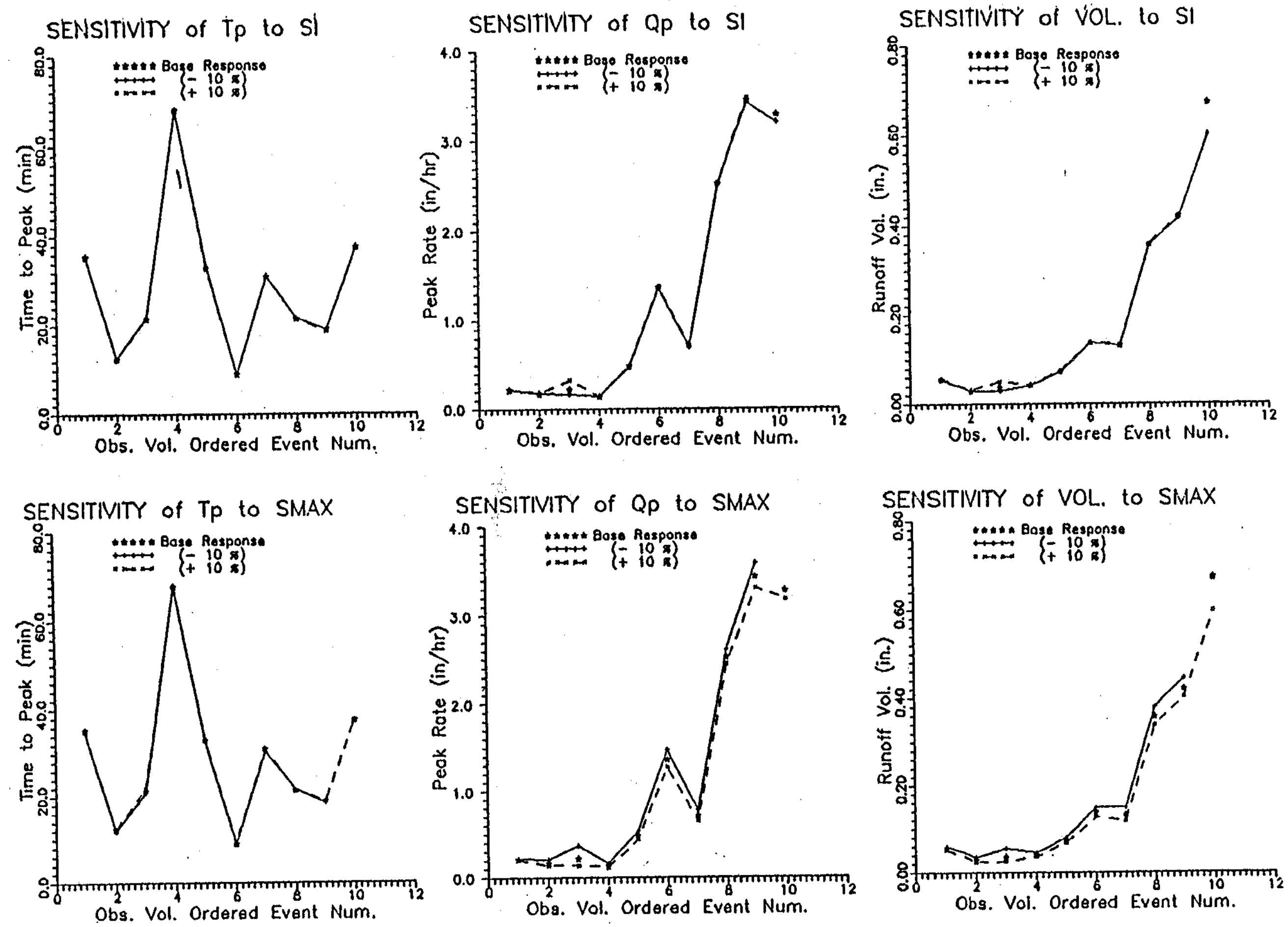

Figure 5.2 Sensitivity of Tp, Qp, and VOL. of Simulated Runoff to a -/+ 10% Perturbation of Selected Model Parameters Over a Range of Ten Events - (Continued)

runoff volume (VOL) are shown. In these figures the base response corresponds to a zero percent parameter perturbation. Solid and dashed lines track the change in runoff response for the -/+ 10% perturbations. The events are ordered from small to large (1-10) based on the runoff volume for each event.

The parameters with negligible impact on the runoff characteristics are the interception (DINTR), the microtopographic roughness term (RECS), as well as channel roughness ($R1_c$) and channel Ks_c. The initial interception values are very small for desert species in LH-106 and, therefore, so are the 10% perturbations. RECS affects the surface area over which infiltration can occur during runoff recession. It is only active on recession when the rainfall rate drops below the infiltration capacity. Because of the way RECS is used in the model, perturbations to it should logically impact runoff volume only. As shown in Figure 5.2, the impact of pertubations of RECS on runoff volume are negligible. Given these results, DINTR and RECS will not be considered for possible calibration parameters. RECS will be set to a value estimated from photogrammetrically measured stereophotos, and DINTR is set to values obtained in the literature for the desert species present (Branson et al., 1981; Tromble, 1983).

The minor effect of channel parameter perturbations results from the small percentage of area that the channels occupy in the basin (less than 2%). Some impact on Tp and Qp by the channel roughness can be detected. It is somewhat surprising that channel roughness changes do not have greater impact, as all of the runoff generated must flow through channel segments to reach the basin outlet.

These findings give an indication of the domination of overland flow processes in runoff generation at this basin scale. This is confirmed by examining the impact on runoff characteristics due to changes to roughness and Ks of overland flow planes ($R1_p$ and Ks_p).

Related to the plane Ks values is the coefficient of variation of Ks_p, (C_v). C_v has significant impact on both Qp and runoff volume (VOL). The sensitivity results for C_v are plotted in both linear and logarithmic scales. The logarithmic plot emphasizes the greater relative impact of C_v on the small runoff events, as was shown in Chapter 2. The other parameters which have significant impact on runoff characteristic are all related to infiltration. The porosity (POR), rock content (ROC), and the initial and maximum relative soil saturation (SI and SMAX) are all used to compute the infiltration capacity of the soil.

The effect of SI and SMAX should be viewed simultaneously as the soil moisture deficit (SMAX-SI) is one of the primary terms defining soil suction. Recall also that the suction term is automatically computed from Ks_p. This was done so that small-scale infiltration variability could be easily treated. By defining the suction term in this way, it can also be removed from consideration as a calibration parameter. In addition, because the suction is highly correlated with Ks_p, including it and Ks_p is likely to lead to identifiability problems.

SI will not be used as a calibration parameter as it will be determined outside of KINEROSR using CREAMS in a repeatable objective manner. The variability of SMAX as determined from textural soils data (Rawls et al., 1982) is relatively small in comparison to other soil hydraulic properties. Because of this fact, coupled with fact that the moisture deficit (SMAX-SI) is the primary parameter of interest, SMAX will also be excluded from calibration. Considering SMAX for calibration, with SI determined independently, would constitute an inconsistent treatment of the two parameters in calibration.

The remaining two parameters, porosity and rock content, have a relatively large impact on runoff when perturbed, but are closely linked with infiltration computations. It is assumed that treatment of the small-scale variation of infiltration in a distribution sense (Chapter 2) will capture the majority of runoff response variation induced by variations in porosity and rock content. Because of the close association between porosity, rock content, and the infiltration computations, these two parameters will also be excluded from calibration to minimize parameter interaction.

To further reduce the possibility of parameter interaction during calibration, a distinction between channel and overland Ks and roughness will not be made. The calibration parameter space will, therefore, consist of three multipliers (three parameters). They are uniform basin multipliers for Ks, C_v, and hydraulic roughness. The roughness multiplier is kept because of its impact on Tp and Qp and because of the subjective nature of the initial estimation. The Ks multiplier is retained because it has significant impacts on both Qp and runoff volume. It also affects the suction term by way of its regression relationship. Ks is also difficult to measure directly, is highly variable, and has been crudely estimated from soil texture measures. The C_v multiplier is also kept in the calibration because of its impacts on Qp and volume and because enough data were not available to define this parameter with a good deal of certainty. The resulting small number of calibration parameters should satisfy the concerns regarding overparameterization mentioned above as well as minimize parameter interaction.

To place the parameter sensitivity analysis in perspective, the sensitivity to rainfall input has also been considered. In the analysis above, measured breakpoint rainfall was obtained from raingage 83. This raingage is approximately 180 m from the centroid of LH-106. Another raingage (384) is located roughly 120 m from the basin centroid. For each of the ten events, the rainfall measured from each of these gages was used to simulate runoff. The fixed set of model parameters (zero perturbation) obtained from fitting event 53 was used for both rainfall input sequences. The variation induced in Tp, Qp, and runoff volume by using the two nearby gages individually is shown in Figure 5.3. In this figure, the observed values are plotted as small stars, and the bands represent the range in variation of Tp, Qp, and volume caused by using different raingages for input.

Figure 5.3 shows that by using the measured rainfall from two adjacent raingages independently, significant variations in runoff characteristics are produced. The two raingages are only about 300 m apart. Typically, for such length scales, rainfall is considered spatially uniform. The results presented in Figure 5.3 indicate otherwise. Table 5.2 contains the total rainfall depths measured for raingage 83 and 384 and summary statistics for each of the events considered. The mean and

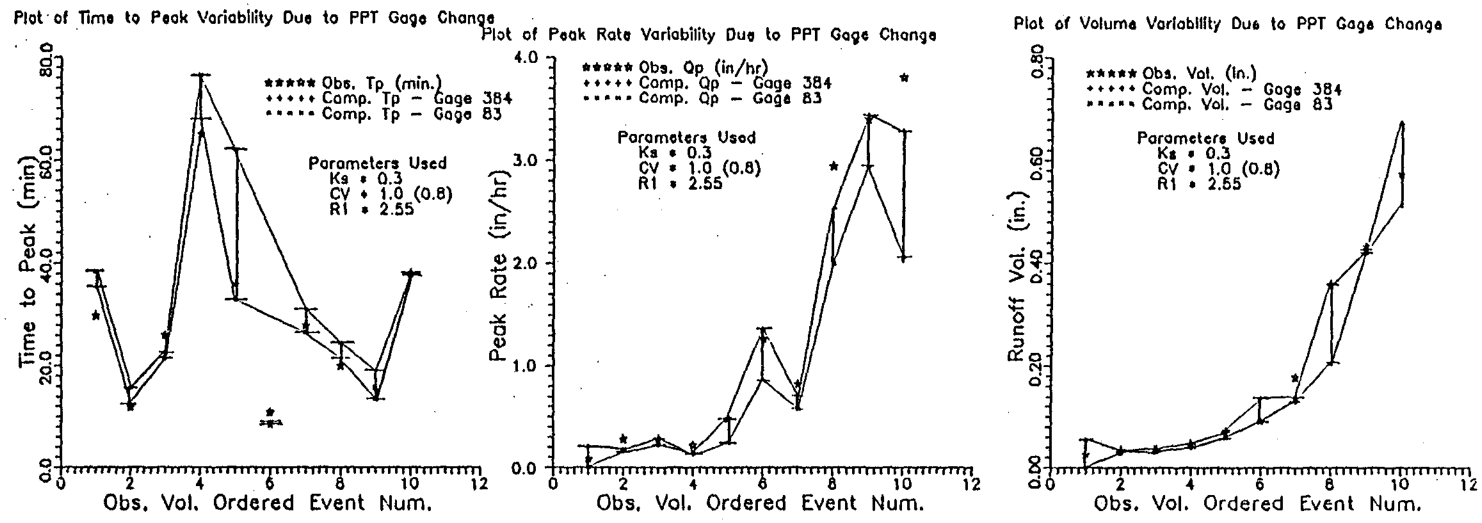

Figure 5.3 Variation in Tp, Qp, and Runoff Volume Caused by Using Rainfall Input from Two Adjacent Raingages (Approximately 300 m Apart)

Table 5.2. Lucky Hills Rainfall Depth Comparisons

Date D/M/Y	Event No.	Total Rainfall (mm) Gage 384	Gage 83
14/ 7/73	48	13.5	15.2
27/ 7/73	49	43.4	39.9
19/ 7/74	50	23.4	26.4
28/ 7/74	51	15.2	18.5
29/ 7/74	52	6.4	7.1
30/ 7/74	53	8.9	12.4
1/ 8/74	54	22.6	27.7
12/10/74	56	8.6	9.7
22/10/74	58	7.9	9.1
29/10/74	59	19.0	20.1
5/ 7/75	60	19.8	18.8
8/ 7/75	61	7.4	7.4
12/ 7/75	62	26.6	27.2
17/ 7/75	63	70.6	72.6
7/ 9/75	64	11.2	13.0
13/ 9/75	64A	17.3	18.5
6/ 9/76	65	24.4	23.6
10/ 9/76	66	9.9	11.4
13/ 7/77	67	10.4	11.4
23/ 7/77	69	8.1	8.9
31/ 7/77	70	12.2	13.5
1/ 8/77	71	10.9	11.7
15/ 8/77	72	26.7	21.6
16/ 8/77	73	12.4	13.7
1/ 9/77	74	27.7	27.7
26/ 9/77	75	26.9	27.9
26/ 9/77	75A	30.2	25.9
	n = 30	Mean = 19.3	20.0
		Stan. Dev. = 13.7	13.2

standard deviations for the rainfall totals are very similar, but percentage differences in individual rainfall totals range as high as 40%. Because interactive infiltration is used in KINEROSR, rainfall intensities rather than rainfall totals are the key input in runoff computations. Greater variation can be expected in intensities due to differencing of accumulated rainfall depths. Differencing is required because the weighing gages used in Walnut Gulch trace total accumulated rainfall on a rotating drum. This trace is digitizied for time and depth coordinates which are then differenced to obtain rainfall intensities. A dramatic illustration of the differences in simulated runoff caused by using the nearby raingages individually is shown in Figure 5.4. This figure shows the measured hyetographs for the two gages and the resulting simulated hydrographs for event 3 used in Chapter 4.

Many factors contribute to spatial variability of rainfall on the scale of 300 m between gages 83 and 384. They include wind effects, slope-aspect effects on gage catch, turbulence caused by the free-standing gage itself, and actual rainfall differences. Several studies have documented these effects in different climatic regimes.

In a Mediterranean climate, Lavee (1986) found differences of 10 to 100% in hydrologic and meteorologic rainfall at the same location. Hydrologic rainfall is measured with a raingage orifice parallel to the ground surface, and meteorologic rainfall is measured with a horizontal raingage orifice (Sharon, 1980). Lima (1989) illustrated the dramatic effect that changes in the incidence angle of rainfall can have

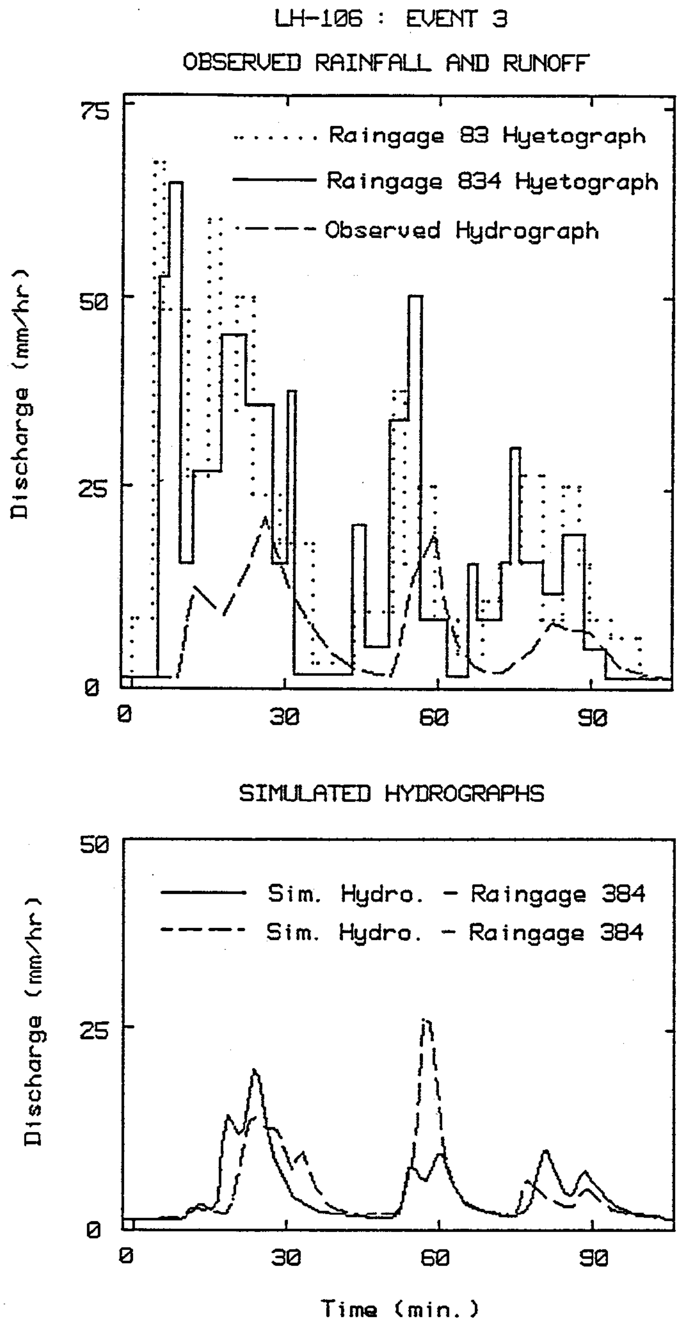

Figure 5.4 Runoff Simulations on LH-106 Using Rainfall from Adjacent Raingages for Event 3 (August 23, 1982)

on overland flow modeling. Lavee (1986) also found that total rainfall varied between 20 and 40% in distances of less than 100 m.

Turbulence effects on rain catch were documented by Neff (1977) and Hanson (1989). Neff used a pit gage adjacent to a normal, above ground, gage installation and found that the above ground gage underestimated total rainfall catch by an average of 15%. The undercatch increased to 30% as wind speed increased. Hanson (1989) found similar results using shielded and unshielded gages. A 15% undercatch in the unshielded gage resulted when surrounding wind speeds were approximately 10 m/s.

In addition to the topographic and meteorologic factors discussed above, mechanical and data reduction errors also contribute to differences in raingage observations. Chery and Beaver (1976) examined Walnut Gulch rainfall data processing and analyzed the measuring accuracy of several data reduction personnel on analog charts of different time and depth scales. For a typical range of storm sizes, they found that the integral squared error (IE) was less than 15% and typically ranged from 5 to 8% where:

$$IE = \frac{\left(\sum_{i=1}^{n} (r_a - r_r)^{1/2}\right)^2}{\sum_{i=1}^{n} r_a} \times 100 : \quad i = 1,2,..,n \tag{5.1}$$

where:

r_a = actual rainfall rate

r_r = read rainfall rate

This measure shows that overall measurement accuracy is quite good but masks inaccuracies in peak rainfall intensity measurement. Peak rainfall intensities determine peak runoff rate to a large extent in a watershed as small as LH-106. Further analysis of the data in Chery and Beaver (1976) shows that the average percentage difference in measured to actual peak rainfall intensity was 20%, with a coefficient of variation of 0.85 and maximum and minimum differences of 50 and 3%, respectively. Shirley (unpublished) examined the accuracy of rainfall intensities obtained by differencing the analog accumulated depth traces. He found that the accuracy decreases when the time interval used to compute rainfall intensities decreases. For 2-minute intensities, the maximum measurement error can be as large as the theoretically correct rate being measured.

Closer examination of Figure 5.4 suggests that actual spatial differences do exist between the two raingages and are not merely an artifact of data processing or wind turbulence. The second peak is the result of a high intensity burst of rainfall on gage 384 that would be missed entirely if gage 83 were used alone. In an attempt to capture this additional information from multiple raingages, a space-time rainfall interpolation algorithm was developed.

In this algorithm, centroid coordinates of all plane and channel model elements, as well as raingages coordinates, are measured and input into KINEROSR. During runoff simulation, the intensities from surrounding gages are linearly interpolated to provide an element intensity. Details of the procedure are presented in Appendix C. Initially, it was not envisioned that rainfall interpolation would be used on this small scale; however, it was anticipated that interpolation would be required for modeling larger scale watersheds (Walnut Gulch subwatershed 11). The effects of incorporation of rainfall interpolation on the small Lucky Hills watersheds will be discussed more fully in the following chapter.

The primary point of the lengthy discussion of rainfall uncertainty is to bound the expectations of the calibration and verification exercise. With the uncertainty in rainfall input due to small- and large-scale variability, in addition to data processing errors, it is impossible to calibrate the model with a degree of certainty greater than the certainty of rainfall input data. This has been pointed out by numerous investigators (Hromadka 1987, 1987a; Hughes, 1989; Hughes and Beater, 1989; Bras and Rodriguez-Iturbe, 1976; Troutman, 1983) but not at the scale of 300 m. Comparison of Figures 5.2 and 5.3 also points out that runoff variations induced by rainfall variability far outweigh the 10% perturbations used in the sensitivity analysis.

This further justifies the selection of only three parameters (multipliers) for model calibration. The sensitivity of modeling results as a function of basin scale is discussed in more detail in the following chapter.

5.3 Model Calibration and Verification

5.3.1 Background

The goal of model calibration and verification for the four watersheds used in this investigation is to acquire confidence in the model and in the ability to make physically realistic interpretations regarding the geometric simplification process over a range of basin scales. The goal is not to find an "optimum" set of parameter multipliers, but a set that is reasonably close to optimum. In fact, Beven (1988a) argued that, because of the extremely complex nature of runoff generation, a true optimum solution and an ultimate validation may never be achieved. He argued that we must operate under a concept of "unknowability".

Given the "unknowability" of the spatial and temporal distribution of rainfall and its significant impact on simulated runoff, the points raised by Beven (1988a) must be given further consideration. The undersampling of the rainfall field often leads to a bias in estimated parameters. Troutman (1983, 1985) noted that spatial sampling errors of the precipitation field resulting from the use of a small number of raingages is the dominating factor causing bias in parameter estimates. The resulting bias can be so great that the final parameter estimates bear no resemblance to physically realistic values but are acting as mere fitting parameters. Final parameters estimates from this investigation will be examined to ensure they are realistic.

5.3.2 Calibration and Verification Data

In keeping with the earlier methodology, a wide range of runoff event sizes and initial conditions will be employed in calibration and verification. There are several reasons for doing so. The first and most obvious reason is to ensure that some degree of generality (at least for basins similar to Walnut Gulch) can be attached to model conclusions and interpretations. Second, every attempt should be made to activate all states of the model so that the resulting parameter estimates used in the model will be unbiased in relation to event size or initial condition (James and Burges, 1982; Sorooshian et al., 1983). The events selected should also include complex, multipeaked hydrographs to more fully test model dynamics as it is relatively simple to fit single-peaked hydrographs (Beven, 1988b).

The calibration and verification events must be independent. In partitioning the events between the two sets, events outside the range of calibration will be held for the verification set. By doing so, the model's predictive capability beyond the calibration range can be assessed (Klemes, 1982). This will test whether the model has more power than regression by embodying causal process knowledge to allow extrapolation.

The importance of obtaining the best possible rainfall and runoff records for selection of the calibration and verification events cannot be overemphasized.

Minimization of observation errors in these records is a must. If significant data errors exist, parameter bias can result in the calibration, just as misrepresentation of rainfall inputs causes bias (Troutman, 1983, 1985). For this investigation, the selected events were chosen from a homogenous time period in which no changes were made to the measuring instrumentation. No major watershed management changes occurred for the period of time selected.

Extremely thorough data checking was conducted for each runoff station and raingage for all of the selected events. If any concerns became apparent during initial data selection from the computer data base, the original analog charts were scrutinized. If further questions persisted, the personnel who collected and processed many of the charts were consulted. It is interesting to note that many of the observation and data processing errors would not have been discovered unless runoff hydrographs and raingage charts from the same storm were examined simultaneously from nearby runoff flumes and raingages. This data redundancy, available in the nested Lucky Hills watersheds, greatly minimized possible observational errors.

A target of obtaining 30 "best possible, minimum error" rainfall-runoff events for each watershed was established. This figure was selected as a compromise between a reasonable number of test events and computational time constraints. The homogenous period of record on Lucky Hills largely constrained the number of useable events as well. Tables containing summary information on all of the rainfall-runoff data events for each of the four watersheds are presented in Appendix A. Frequency histograms of event runoff volume and peak runoff rate for 30 selected events on LH-106 are presented in Figure 5.5 as a typical example of the data distributions. The histograms illustrate the large percentage of small events in the selected set. A set of 27, 27, and 25 events were selected for LH-106, LH-102, and LH-104, respectively. The set consisted of all events recorded in the homogenous time period that were not rejected due to possible errors and met a minimum runoff criteria. A minimum runoff volume of 0.25 mm over the basin was selected. This depth of runoff over the basin is consistent with the measuring resolution of the raingages. Trying to discern runoff dynamics from smaller events only invites trouble in parameter estimation, as observation error most certainly will dominate the rainfall-runoff simulation.

To satisfy the requirements of full model testing over a range of event sizes and initial conditions, a matrix of relative event size versus dry to wet initial conditions was established to aid in calibration event selection. The initial set of 30 events was ranked by observed runoff volume and split into three sets of ten corresponding to small, medium, and large events. The primary purpose of examining events with different initial conditions is to ensure full exercise of suction-related infiltration dynamics. Another way of exercising this model component is to inspect rainfall hyetographs and select storms which peak early or late. The suction terms will be most important for dry initial conditions and early-peaking storms and least important for wet initial conditions and late-peaking storms. Therefore, both initial relative soil saturation (SI) values obtained from CREAMS and storm patterns were used in selecting events covering a range of conditions for fully activating

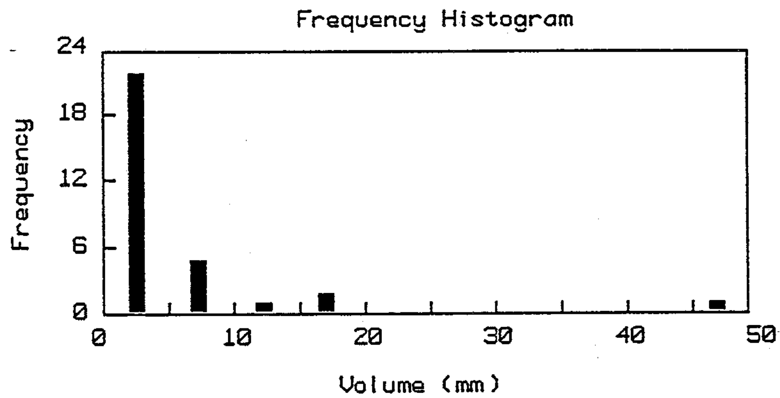

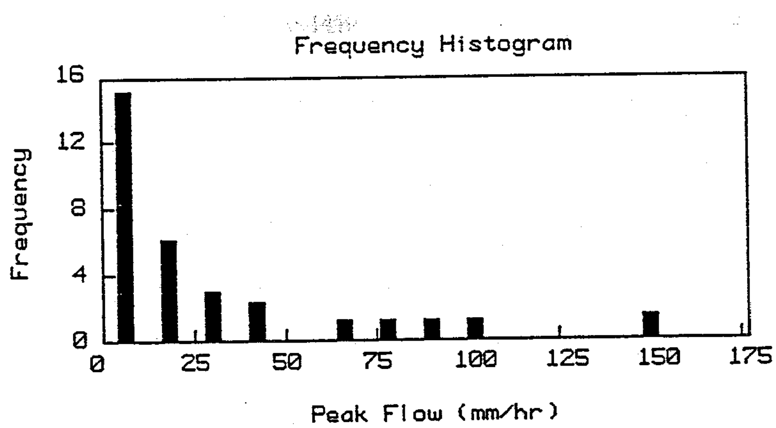

Figure 5.5 Frequency Histograms of Runoff Volume and Peak Runoff Rate for LH-106 for the Selected Calibration and Verification Events

infiltration dynamics. A schematic of the selection matrix with rough storm pattern sketches for LH-106 is shown in Figure 5.6. In addition to the nine calibration conditions depicted in Figure 5.6, event 53 was added at the (medium storm size - wet initial condition) location. Because of the close proximity of LH-102 and LH-104, the same events were selected for calibration in these watersheds. One event was dropped from the LH-104 calibration set after an error was detected and calibration proceeded with nine events. The remaining events were held for independent verification.

The same strategy was employed for calibration event selection for subwatershed 11 (WG11, area = 631 hectares). However, due to the large spatial scales, all of the combinatorics of possible initial conditions and thunderstorm cell locations could not be covered with ten calibration events. The type of conditions found in WG11 that differ from the Lucky Hills watersheds are storm center location (lower or upper portion of the basin) and dry or wet initial channel conditions, as channel losses are very important in WG11. These limitations are recognized, but to allow ready comparison of results across all basins, ten events were used for calibration in WG11 as well.

5.3.3 Measuring Model Performance

Numerous measures have been suggested to gauge model performance. Investigations of various measures have been presented by Aitken (1973), James and Burges (1982), Nash and Sutcliffe (1970), McCuen and Snyder (1975), Willmott

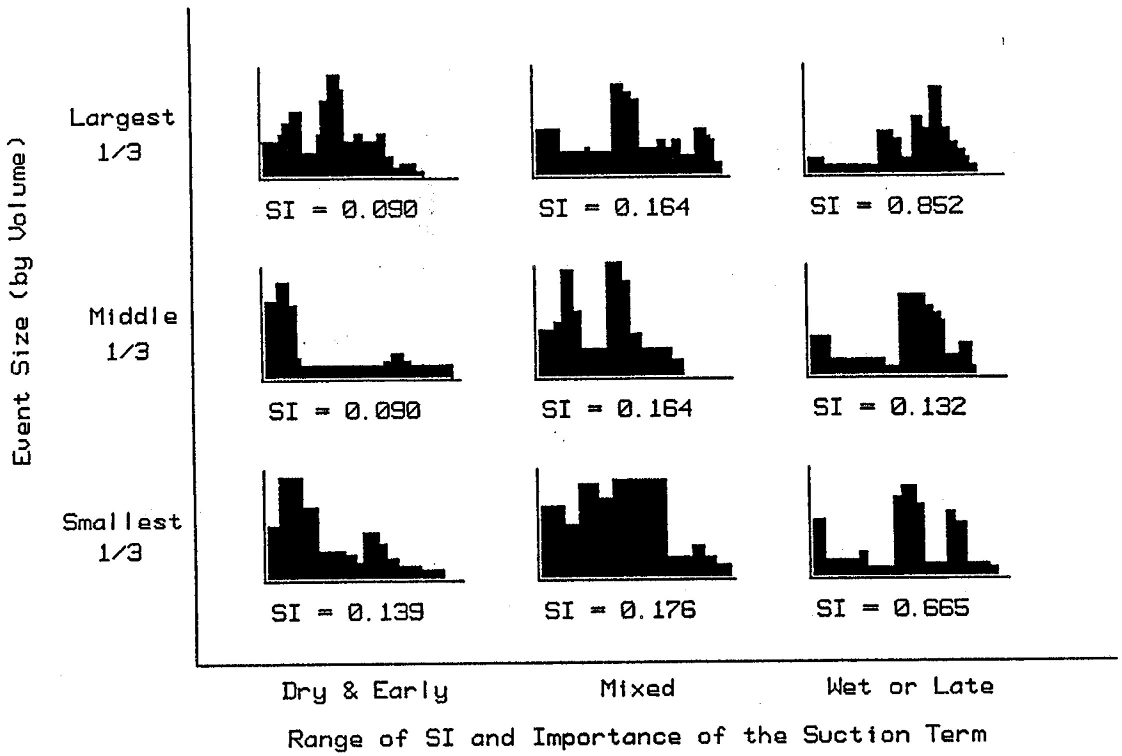

Figure 5.6 Calibration Event Selection Matrix for LH-106

(1982), and Willmott et al. (1985). Although many measures can be used, Martinec and Rango (1989) cautioned that using too many criteria can cause difficulty in assessing model performance. The primary measure selected to assess model performance in this study is the coefficient of efficiency, E, introduced by Nash and Sutcliffe (1970). The coefficient is computed as follows:

$$E = 1 - \left[\frac{\sum_{i=1}^{n} (\hat{Q}_i - Q_i)^2}{\sum_{i=1}^{n} (Q_i - \overline{Q})^2} \right] \quad : \quad i = 1,2,..,n \qquad (5.2)$$

where:

Q_i = simulated model runoff summary variable

Q_i = observed runoff summary variable

Q = mean of Q_i for all events $i = 1$ to n.

Q_i can be time varying discharge, event runoff volume, event peak runoff rate, or time to peak rate. For this study only event runoff volume and event peak runoff rate will be used for Q_i in Equation (5.2).

The coefficient of efficiency was selected because it is dimensionless and is easily interpreted. If the model predicts observed runoff with perfection, $E = 1$. If $E < 0$, the model's predictive power is worse than simply using the average of observed values Q_i. For this study, the mean of the runoff summary variable will be computed from the Q_i values separately in the calibration and verification event subsets. Martinec and Rango (1989) stressed that the mean for the period of interest should be used and not a long-term mean (continuous simulation in their case) as this will artifically improve the efficiencies. This measure has also been used by other investigators to assess event model performance on Walnut Gulch (Hughes, 1989; Hughes and Beater, 1989) and other small experimental watersheds (Loague and Freeze, 1985; Loague, 1986; Loague, 1990). Comparison of results from this study with other investigations will be facilitated by using this measure.

In addition to this measure, the usual unweighted squared difference measure was computed for the entire event hydrograph allowing for a time shift between observed and simulated hydrographs. Timing-based measures such as time to peak and differences in observed and simulated runoff without allowing a time shift were not computed for the following reason. The response time of the small Lucky Hills watersheds is on the order of minutes for a high-intensity rainfall event. Because the raingage and runoff clocks are not the same, the error in clock time can be on the order of the response time. The time shift in computing the least squares differences was introduced to minimize the clock timing error, as very large penalties are introduced during a steep hydrograph rise for very small timing differences.

The primary runoff variables used in model calibration and verification are total event runoff volume and peak runoff rate. More weight will be given to runoff volume for determining infiltration related multiplier parameters. Peak runoff rate will be given more weight in determining the roughness multiplier. For overall consideration, preservation of runoff volume will be given highest priority. For the small watersheds, this should preserve peak rate relatively well, as a high correlation exists between runoff volume (V) and peak rate (Qp). For the selected LH-106 runoff events, whose frequencies of V and Qp are shown in Figure 5.4, a correlation coefficient of 0.9 exists between V and Qp, with a standard error of estimate of 16 mm/hr in the dependent variable Qp. For the ten calibration events on each watershed, the coefficient of efficiency (E) will be computed for both V and Qp. The same statistic is used to assess the model simulations of runoff volumes and peaks of the verification events. For the verification events, the model is assessed for both forecasting efficiencies (E_f) and prediction efficiencies (E_p). Forecasting efficiencies are computed using matched sequences of simulated and observed runoff variables. Prediction efficiencies are computed after the simulated and observed runoff variables are independently ranked. This measure is more useful in assessing the model's ability to reproduce typical runoff distributions for frequency analysis. Forecasting efficiency is the more rigorous of the two tests.

Although the coefficient of efficiency is a widely used measure with easily interpretable properties, it is not without its shortcomings. As Loague (1990) pointed out, large runoff event variables are more heavily weighted, producing better efficiencies if large events are simulated with more accuracy than small events. However, if large events are avoided and a narrow range of event sizes is used, the coefficient can also artificially penalize the user. Imagine a set of events that all have the same runoff volume. The denominator in Equation (5.2) will vanish, resulting in E = -∞, even if the model simulates runoff almost perfectly. The smaller the observed data variance [a small denominator in Equation (5.2)], the better the model must perform to achieve comparable efficiencies. A slight bias toward better simulation of large events is not considered a major problem because they account for a large percentage of total runoff volume and often pose greater management problems. Therefore, Equation (5.2) will be used to compute E over the range of events selected with the bias toward large events kept in mind. Khan (1989) offered a methodology for model evaluation of bands of runoff ranges, but a great deal of data is required and the method cannot be used easily in calibration.

The mean and standard deviation of simulated V and Qp will also be presented for comparison with the same statistics for the observed data. Formal hypothesis testing for comparing observed and simulated distributions will not be made given the small samples used in this study, the required underlying distribution assumptions, and the arbitrary selection of confidence levels required. The means and standard deviations are presented for qualitative assessment and are only intended to provide additional summary information to the computed efficiency coefficients.

5.3.4 The Search for Acceptable Model Parameters

Efficiency coefficients for V and Qp are used as the objective functions to judge model performance at various parameter locations. To reiterate, the parameters in this study are the uniform multipliers M_K, M_C, and M_R applied to the distributed, field estimated, values of Ks, C_v, and R1 (roughness), respectively. The parameter space is, therefore, three-dimensional, and the goal is to find a set of parameter multipliers within this space that will acceptably reproduce observed runoff when they are applied to their respective field estimated model parameters.

Numerous algorithms exist to find optimum parameters for a specified objective function. For nondifferentiable functions, often encountered in rainfall-runoff models, a direct search algorithm such as the simplex method presented by Nelder and Mead (1965) is commonly employed. However, these algorithms are not without their problems. The values of final, "optimal" parameters obtained by the algorithm are often a function of the starting location, step size, and stopping criteria. Many times local, instead of, global maxima (for the objective function used here) are obtained. Selection of an inappropriate objective function for the error data structure and poor model structure with significant parameter interactions can also cause great difficulty for many optimization algorithms (Sorooshian and Dracup, 1980; Sorooshian and Gupta, 1983).

Remember that the goal of model calibration in this study is not to find the optimum set of parameter multipliers but to find a near optimum set that will ensure that the model can be used and interpreted with confidence. Beven (1989) argued that an "optimum" model is unlikely given the watershed complexities rarely addressed in either data collection or model structure. Given these difficulties in application of optimization algorithms, an "intelligent" grid search for acceptable model parameters was undertaken for this study. Intelligent in this situation implies a redefinition of the search space based on results from simulations in a small sample of the parameter space. To examine response surface characteristics, a griding procedure must be conducted anyway. Indeed, Beck (1987) pointed out the failure of many constrained optimization procedures and argued for griding out the entire response surface with the availability of more computing power. Beck goes on to note that there will be relatively few rewards by enhancing algorithmic optimization methods.

The subgrid search was carried out for each of the watersheds to obtain acceptable parameter multipliers M_K, M_C, and M_R. Table 5.3 contains the final multipliers obtained for each watershed. The following section addresses the acceptability of these multipliers. With regard to Troutman's (1983, 1985) concerns, it should be stressed that in all cases when the multipliers are applied to their respective distributed, field-estimated, parameters, realistic parameter estimates are obtained. The resulting Ks values ranged from 2.4 to 19.8 mm/hr for Ks, 0.02 to 0.09 for Manning's roughness, and from 0.8 to 1.0 for C_v. The response surface for M_R = 2.2 of LH-104 calibration efficiencies for V and Qp are show in Figure 5.7. The plots indicate that some interaction between M_K and M_C does exist. It should also be noted that the best combination of M_K and M_C for runoff volume (0.55 and 0.8) does not coincide with the best combination for peak rate. However, the Qp efficiency response surface is very flat and still yields an efficiency of approximately 0.97 for M_K = 0.55 and M_C = 0.8. M_R was selected primarily on the basis of Qp

Table 5.3. Final Multipliers (Calibration Parameters)

Basin	M_K	M_C	M_R
LH-106	0.3	1.0	1.0
LH-102	0.55	1.0	2.2
LH-104	0.55	0.8	2.2
WG11	1.325	1.0	1.25

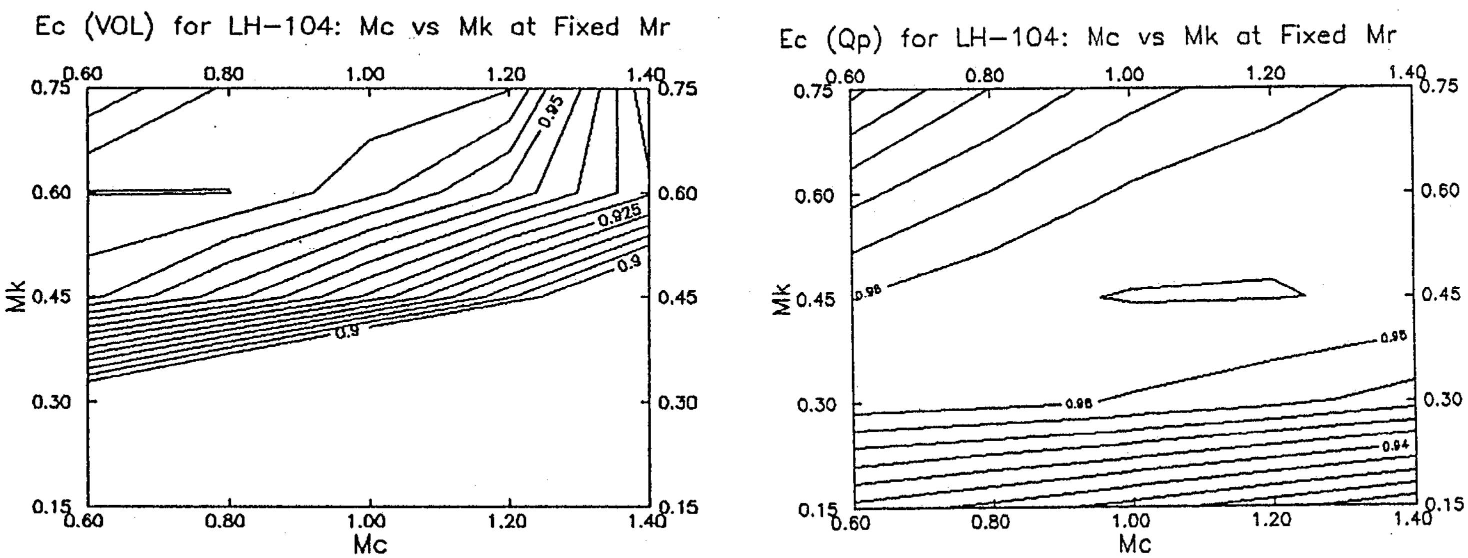

Figure 5.7 Response Surface Plots of Volume and Peak Rate Calibration Efficiency at Fixed M_R for LH-104

efficiencies. Figure 5.8 shows the variation in volume and peak rate efficiency as a function of the roughness multiplier M_R for fixed M_K and M_C. The figure illustrates that M_R has very little effect of runoff volume as was shown in the sensitivity analysis.

Figures comparable to 5.7 and 5.8 were examined for the other watersheds to aid in the selection of final multipliers. A more detailed examination of these figures is carried out in the following chapter when watershed response as a function of basin scale is discussed. By examination of the efficiencies over a range of the multiplier parameter space, a set of multipliers for each watershed has been selected. The question of acceptability of these parameter remains. Does the model reproduce observed runoff behavior when the final multipliers are applied to the distributed field estimated model parameters?

5.3.5 Verification of Model Acceptability

Calibration and verification efficiencies for observed and simulated runoff volumes and peak rates are shown in Table 5.4 for each of the watersheds. Efficiency coefficients for both forecasting and prediction are included. Table 5.5 contains summary statistics and average sum of squared differences (allowing for a time shift) for the watersheds. Examination of the tables supports the conclusion that the model performed very well for the Lucky Hills watersheds and marginally well for WG11 for independent verification event sets.

Note that the calibration efficiencies for WG11 are quite good. Possible reasons for the degradation of model results during WG11 verification were alluded

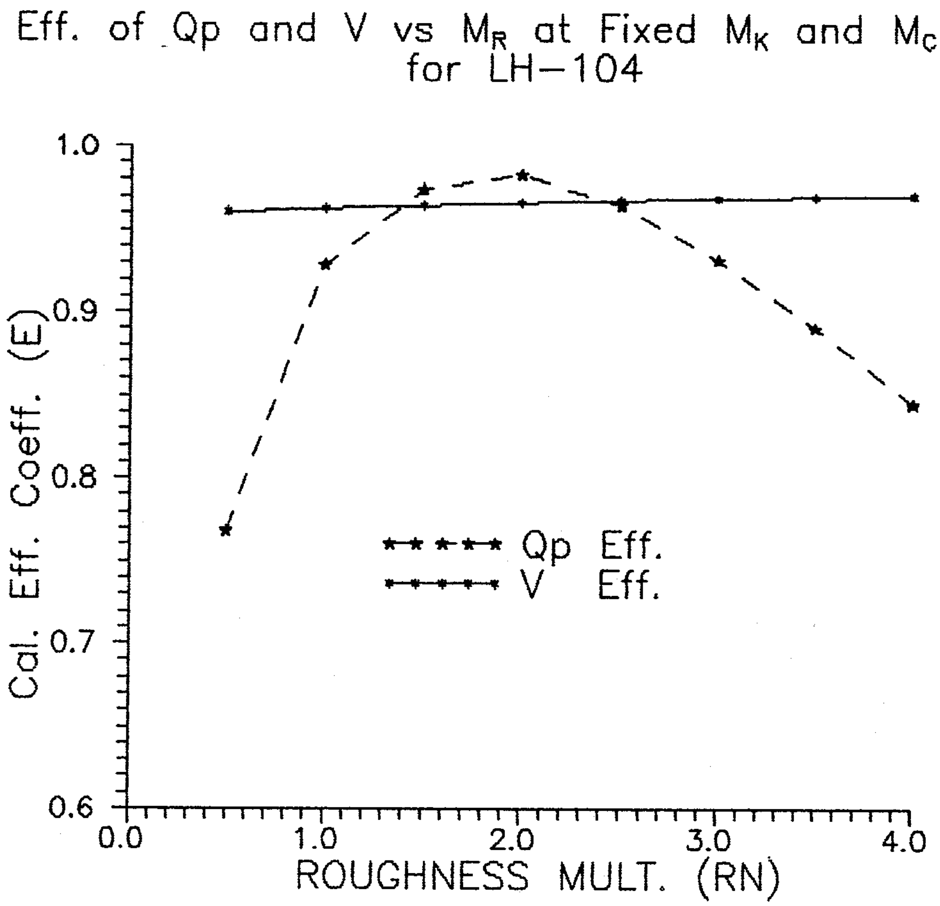

Figure 5.8 Response of Volume and Peak Rate Calibration Efficiency to M_R for Fixed M_K and M_C for LH-104

Table 5.4. Calibration and Verification Forecasting and Prediction Efficiencies for Runoff Volume and Peak Rate for All Study Basins

		Calibration Efficiencies				Verification Efficiencies			
		E_f		E_p		E_f		E_p	
Basin	Area (ha)	V	Qp	V	Qp	V	Qp	V	Qp
LH-106 n_c = 10 n_v = 17	0.36	0.98	0.95	0.98	0.98	0.98	0.79	0.98	0.83
LH-102 n_c = 10 n_v = 17	1.46	0.97	0.97	0.97	0.97	0.93	0.93	0.94	0.95
LH-104 n_c = 9 n_v = 16	4.40	0.97	0.98	0.97	0.98	0.99	0.96	0.99	0.97
WG11 n_c = 10 n_v = 20	631	0.86	0.84	0.96	0.90	0.49	0.16	0.70	0.25

n_c = number of calibration events
n_v = Number of verification events

Table 5.5. Mean and Standard Deviation for Volume and Peak Rates and Average Sum of Squared Deviations for Calibration and Verification Events Sets for All Study Basins

Basin	Area (ha)	Event Set	Type	Num. of Events	V (mm) Mean	V (mm) S.D.	Qp(mm/hr) Mean	Qp(mm/hr) S.D.	Average Sum of Sq. Dev. $(mm/hr)^2$
LH-102	0.36	Calib.	Obs.	10	4.74	5.03	34.2	36.8	
			Sim.	10	4.78	4.98	35.6	36.8	520
		Verif.	Obs.	17	6.22	11.4	27.1	36.7	
			Sim.	17	6.96	12.1	33.3	38.5	1170
LH-102	1.46	Calib.	Obs.	10	4.57	4.48	27.6	27.8	
			Sim.	10	4.36	4.61	26.5	27.7	258
		Verif.	Obs.	17	6.01	9.88	24.6	26.6	
			Sim.	17	6.76	12.1	25.3	31.1	688
LH-104	4.40	Calib.	Obs.	9	4.27	4.49	28.0	30.1	
			Sim.	9	4.44	4.99	24.8	29.3	343
		Verif.	Obs.	16	6.37	11.9	26.3	34.6	
			Sim.	16	6.76	12.3	23.0	30.2	897
WG11	631	Calib.	Obs.	10	2.54	1.88	4.37	4.25	
			Sim.	10	2.39	2.03	4.04	3.72	75
		Verif.	Obs.	20	2.16	1.78	4.30	3.25	
			Sim.	20	1.89	2.62	3.78	5.52	110

to earlier. In WG11, significant large-scale rainfall variability is present in most rainfall events and channel losses are much more important. With a small calibration set of ten events, many of the combinations of storm pattern and channel initial conditions as well as storm size and basin initial conditions could not be covered. Thus, the calibrated parameters may not have captured sufficient information to allow modeling of events in the verification set that are distinctly different from those in the calibration set. It should also be noted that the level of field data collection in WG11 was not as intensive as in the Lucky Hills watersheds due to manpower constraints. This, of course, leads to greater uncertainty in the initial parameter estimates. Additional discussion of model performance as a function of basin scale in presented in Chapter 6.

The modeling results presented here are also compared to other modeling efforts using a distributed kinematic wave type model on another USDA Agricultural Research Watershed and on Walnut Gulch with a conceptual model. Loague and Freeze (1985), Loague (1986), and Loague (1990) did extensive work on the R-5 watershed (area = 0.1 km^2) near Chickasha, Oklahoma. Their best forecasting efficiencies for volume and peak rate were 0.25 and 0.71, respectively, when calibration with Ks adjustments were done. The calibration in this study used three parameters which would help improve efficiencies. However, by examining the final parameter multipliers used for LH-106 (Table 5.3), it is apparent that only one parameter (M_K) was adjusted in the calibration, yet E_f of 0.98 was obtained for verification volumes in this study. Loague (1990) obtained slightly improved results when additional soils information was incorporated and no calibration was done. R-5 is significantly different from Walnut Gulch, and some data problems were encountered by Loague (1990); therefore, comparisons to the present study's results may not be entirely fair.

More comparable results can be found in Hughes and Beater (1989), who used data from six Walnut Gulch watersheds (43 large events), with a lumped and semidistributed conceptual model. Their best forecast efficiencies were -0.02 and 0.01 for the lumped and semidistributed version of their more complex model that did not allow parameter adjustment for verification events. Using model parameters predicted by basin and climate measures while still allowing calibration, Hughes (1989) obtained a calibration and verification efficiency of 0.07 and 0.03, respectively, for Walnut Gulch runoff data. It is not clear how Hughes and Beater (1989) and Hughes (1989) computed efficiencies, but due to the dimensionless nature of the measure, it still provides a fair indication of their modeling results on Walnut Gulch watersheds.

The summary statistics above demonstrate that the model simulations are, by and large, very good for the Lucky Hills watersheds and relatively good (in comparison to other studies) for WG11. The efficiencies and statistics presented in Tables 5.4 and 5.5 embody a great deal of information for the entire calibration and verification event sets. To more fully evaluate model performance, visual presentation of individual events is offered. Visual analysis, although subjective, is still a valuable tool for model evaluation Willmott et al. (1985).

Figures 5.9 to 5.12 contain scatter plots of observed versus simulated runoff volumes and peak rates for the calibration and verification event sets. The figures are arranged from small (Figure 5.9) to large (Figure 5.12) basin size. These figures further confirm the conclusions drawn above regarding model performance for the Lucky Hills and WG11 watersheds. It should also be noted that the largest runoff event on record for Lucky Hills (Event 63), which is included in the verification set, is well predicted for all the Lucky Hills watersheds. For these basin scales, the model has extrapolation capability as it simulates runoff from events well outside the calibration range. The scatter plots for the WG11 verification set show a trend of underprediction for small events and over prediction for large events. However, the WG11 simulations cannot be dismissed outright as being unacceptable.

For yet a more detailed model assessment, individual hydrographs for the worst and best (near best in some cases) events in the calibration event set are presented. For all of the Lucky Hills watersheds, the worst simulation occurred for event 73. This is also the smallest event, by observed runoff volume, included in the calibration set. The worst and best simulations on WG11 occurred on July 24, 1986 and on August 4, 1980, respectively. The worst simulation on WG11 also corresponded to the smallest event of the calibration set. A single best event on all of the Lucky Hills watersheds could not be selected; therefore, event 62 was selected as a "near best" event for the three Lucky Hills watersheds. A single "near best" event is desired in order that comparisons of the hydrographs can be made across a range of basin scales in Lucky Hills. In addition, for the LH-106 and LH-102 worst and best

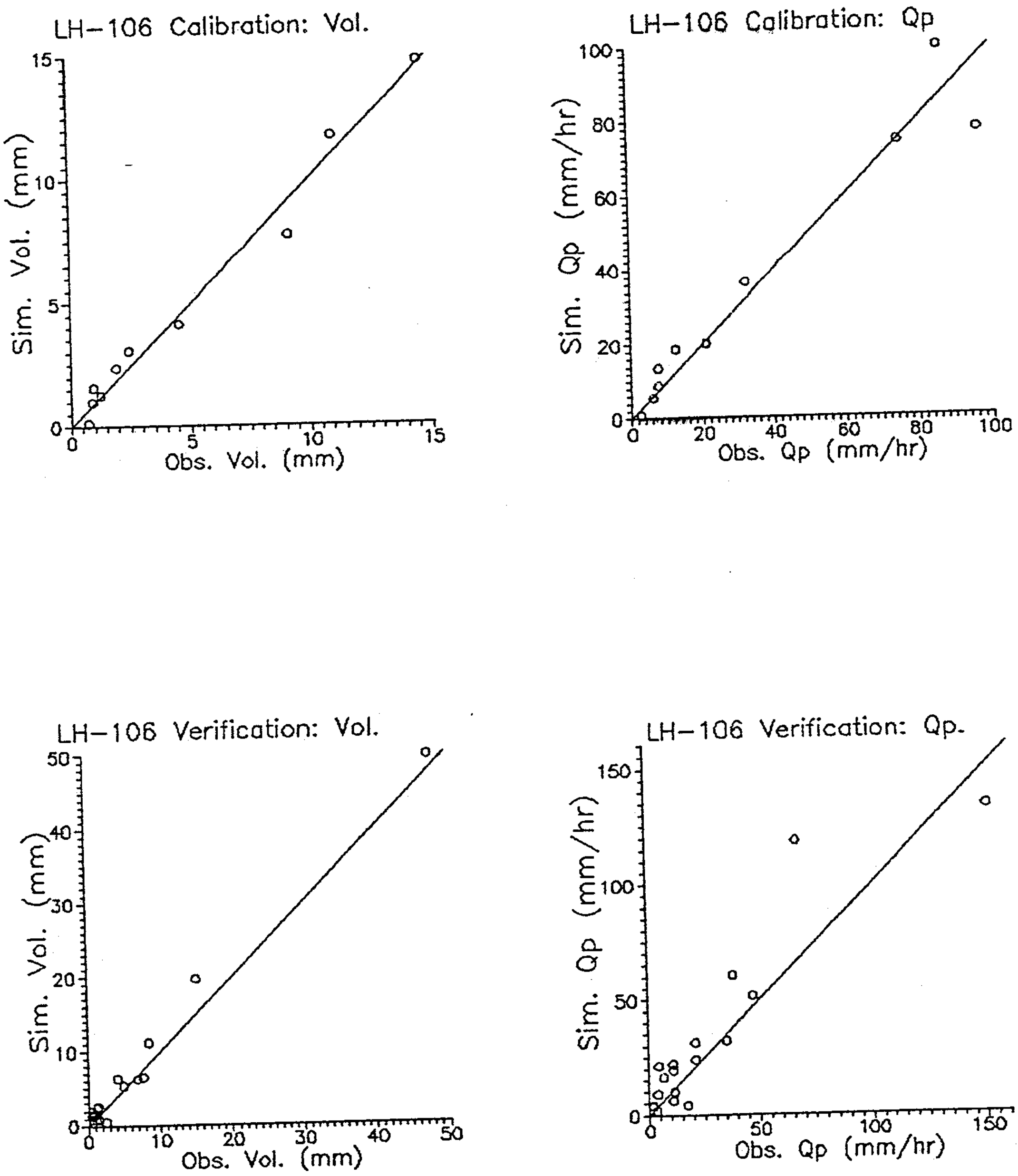

Figure 5.9 LH-106: Observed Versus Simulated Volumes and Peak Rates for Calibration and Verification Event Sets

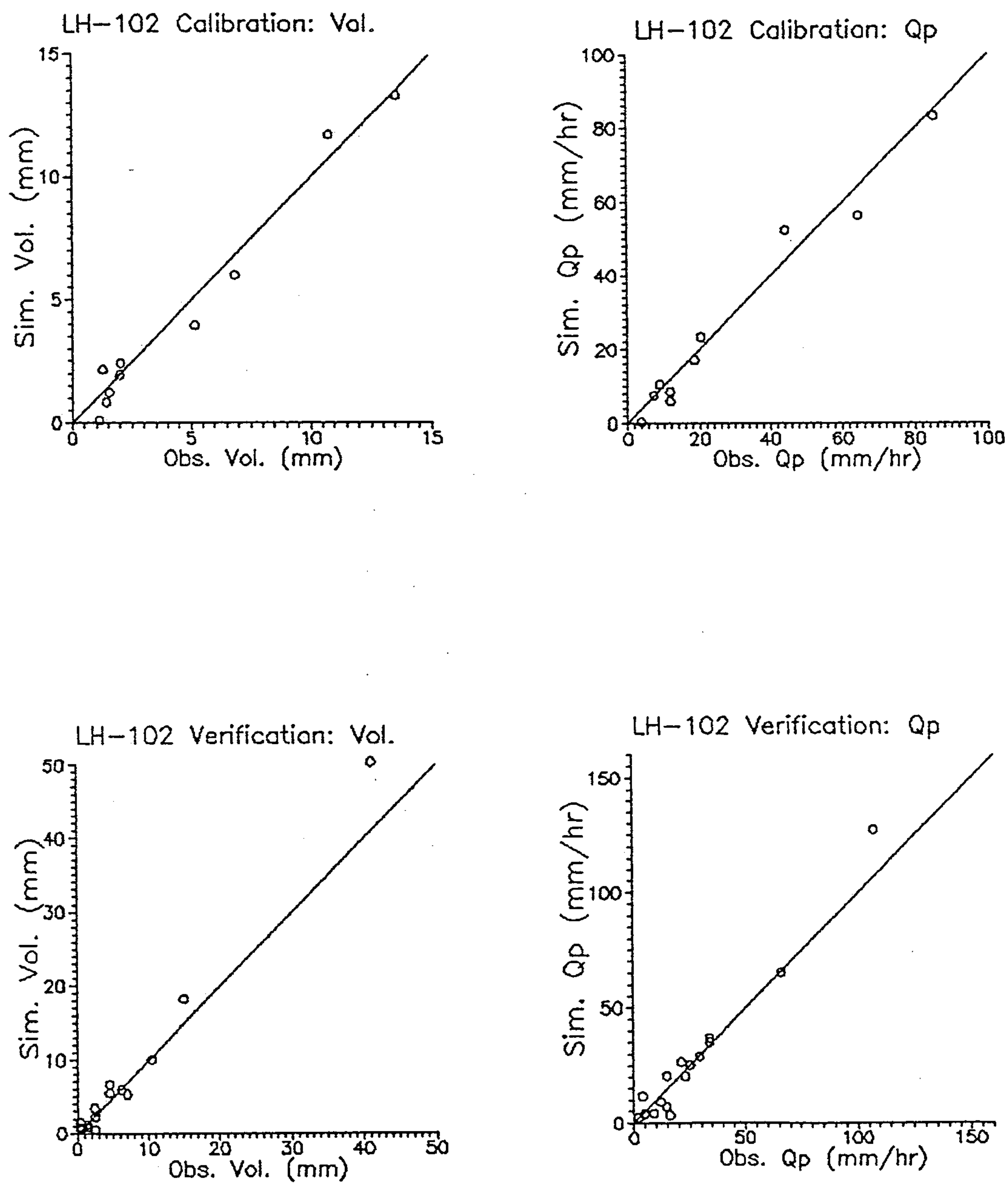

Figure 5.10 LH-102: Observed Versus Simulated Volumes and Peak Rates for Calibration and Verification Event Sets

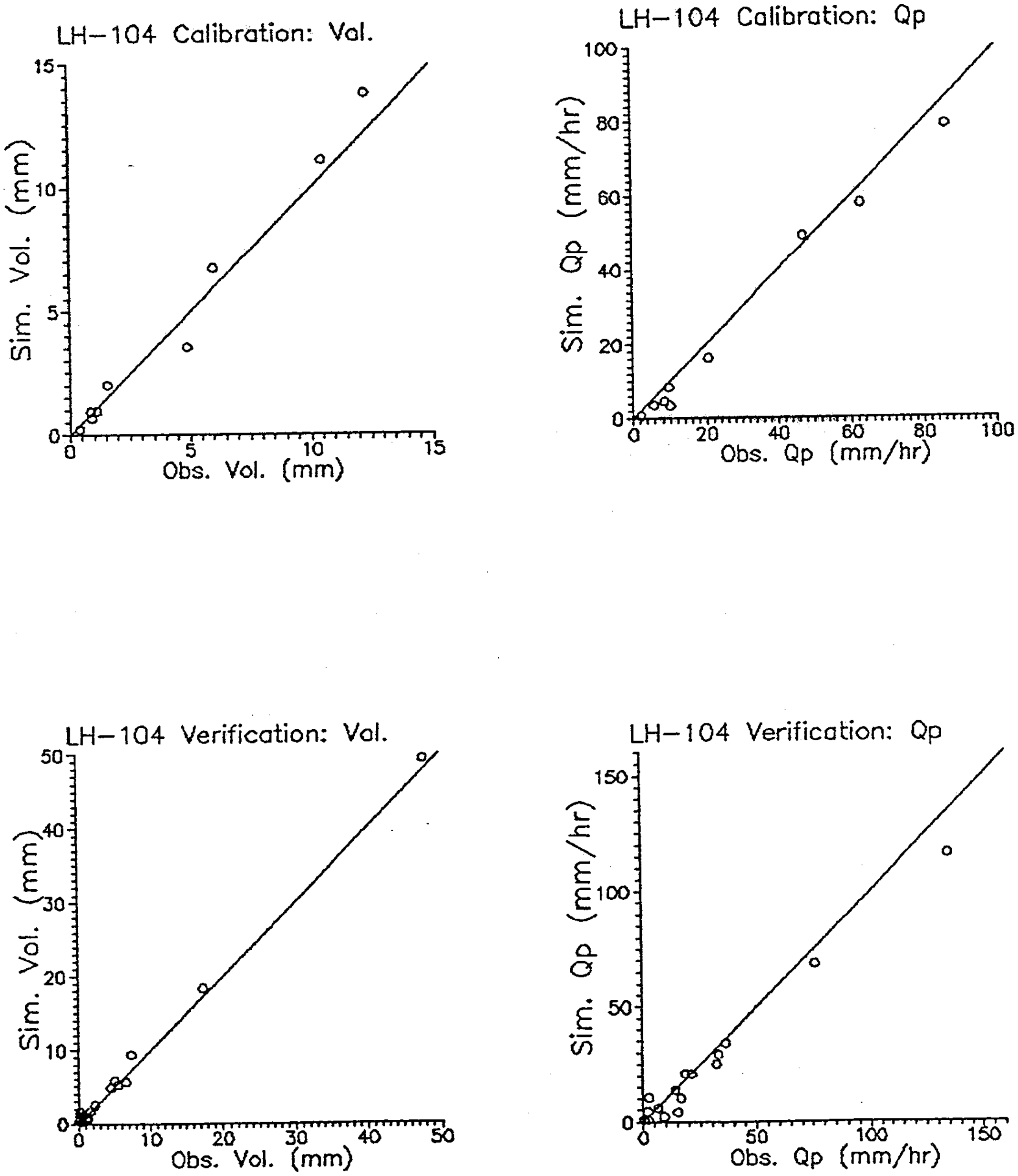

Figure 5.11 LH-104: Observed Versus Simulated Volumes and Peak Rates for Calibration and Verification Event Sets

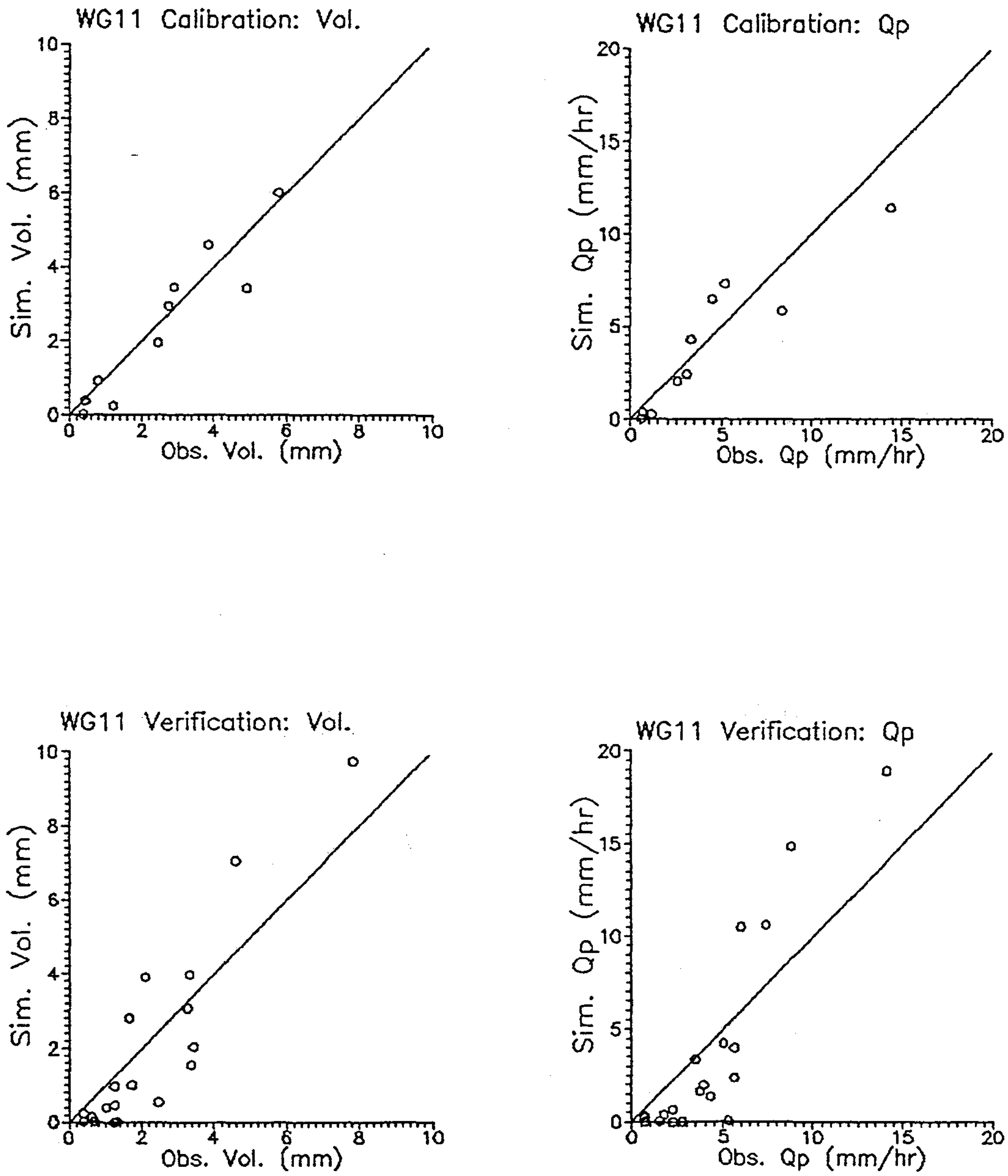

Figure 5.12 WG11: Observed Versus Simulated Volumes and Peak Rates for Calibration and Verification Event Sets

plots, the corresponding model simulations using the final parameter multipliers from LH-104 are presented. Because LH-106 and LH-102 are subbasins of LH-104, this will allow visual assessment of internal model consistency.

The best and worst calibration simulation hydrographs for all the basins, in ascending basin drainage area, are shown in Figures 5.13 to 5.16. Timing errors of approximately eight to ten minutes or less are irrelevant in the Lucky Hills watershed, as clock error could easily be this large. The best or near best simulations occur for the larger events for all of the watersheds, and the worst simulations occur for the smallest calibration event for all basins. These small events have observed runoff volumes and peak rates that are smaller by more than a factor of ten than any of the largest three events in the calibration set. For events of this size, the uncertainty associated with measurement error can become a large percentage of the observed runoff. The nonlinearities in the infiltration process will also tend to dominate the rainfall-runoff transformation for such small events as was illustrated in Chapter 2.

The important issue of internal model accuracy can be partially addressed by examining the third best simulations in LH-106 and LH-102 shown in Figures 5.13 and 5.14. In these figures, the hydrographs obtained from using the final LH-104 multipliers on the internal LH-106 and LH-102 basins are illustrated. For the larger event (#62), very good internal simulations were obtained using the overall, larger LH-104, basin parameter multipliers. The same cannot be said for the small event (#73), as simulations were very poor for this event even when using parameter

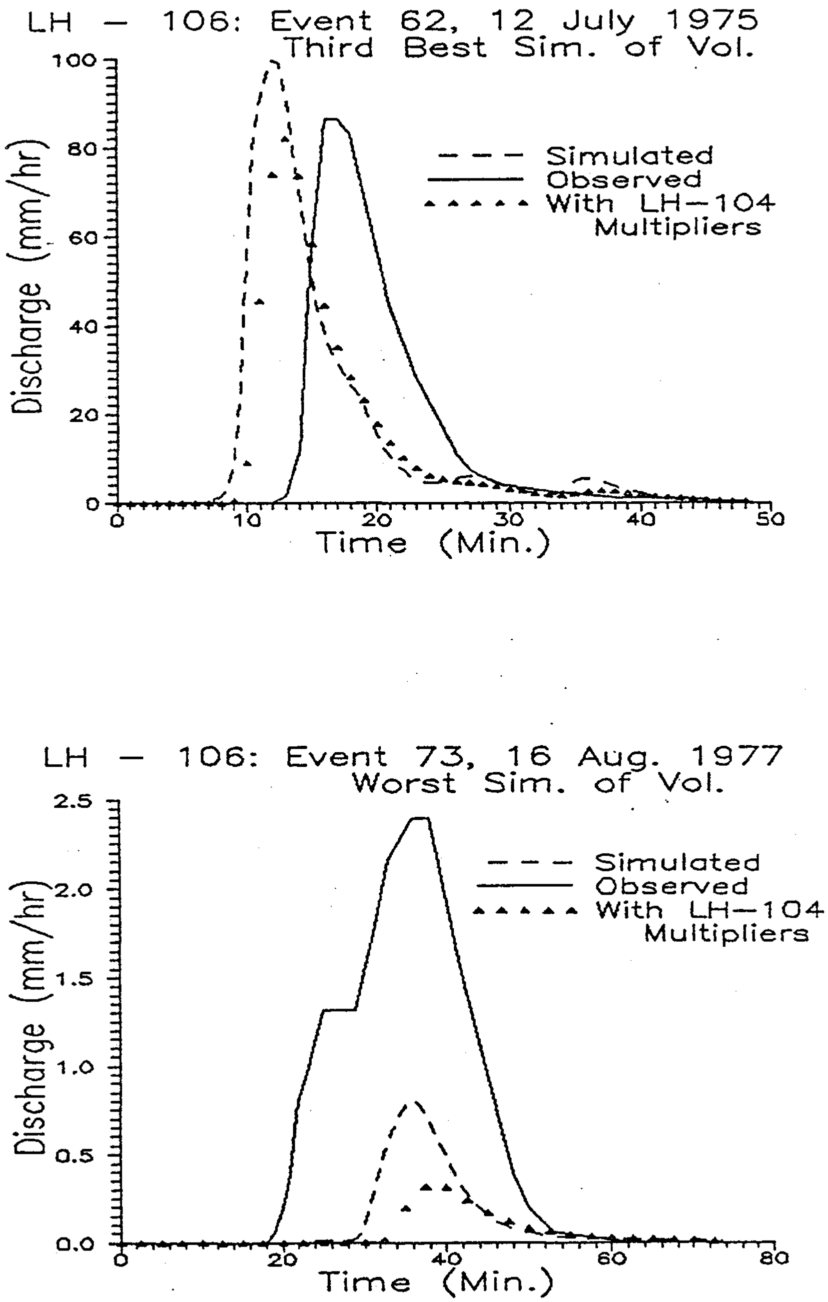

Figure 5.13 LH-106: Third Best and Worst Calibration Hydrographs Based on Volume and Comparable LH-104 Model Hydrographs Using LH-104 Multipliers

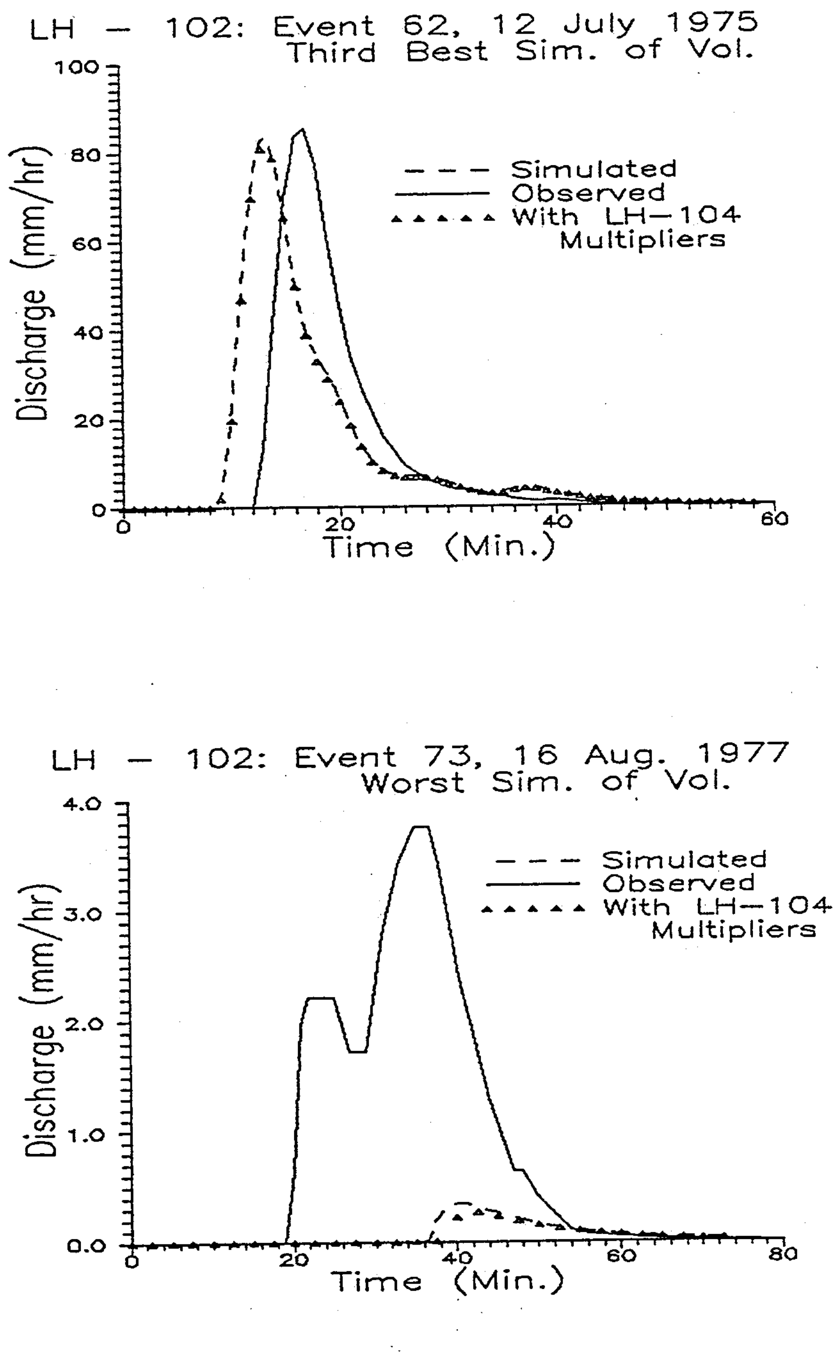

Figure 5.14 LH-102: Third Best and Worst Calibration Hydrographs Based on Volume and Comparable LH-104 Model Hydrographs Using LH-104 Multipliers

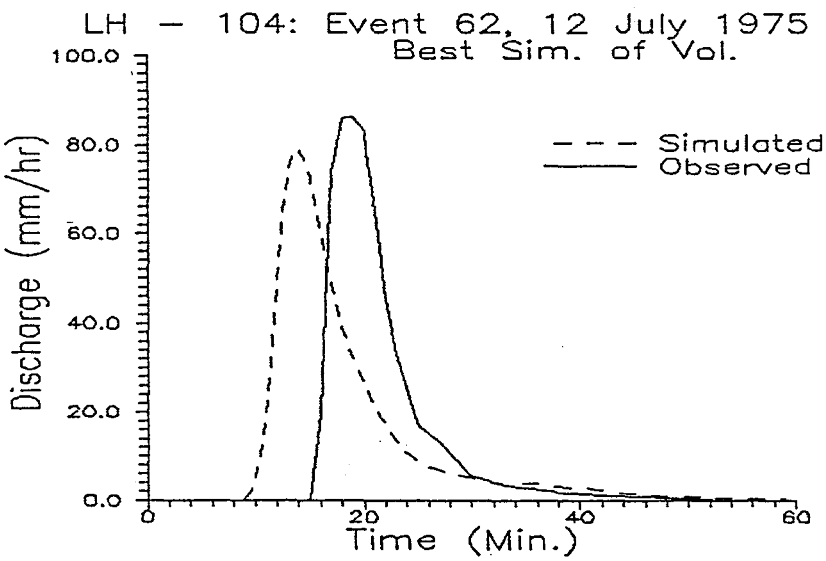

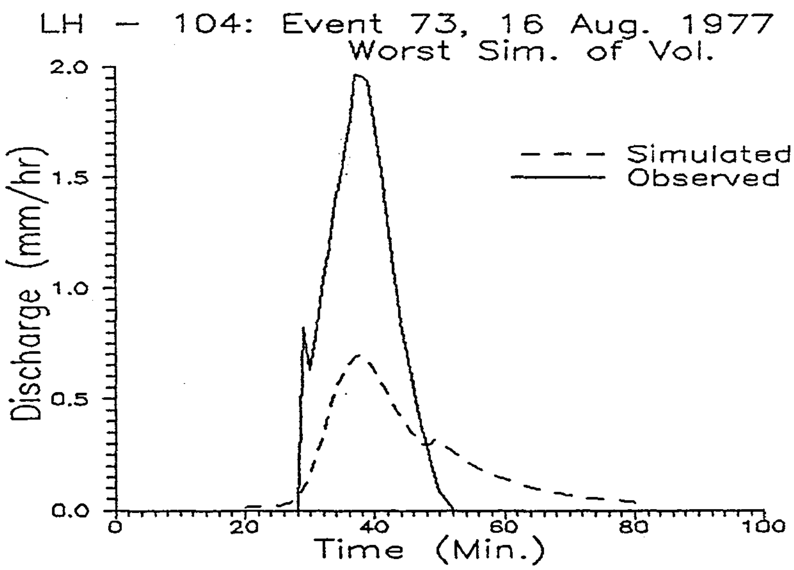

Figure 5.15 LH-104: Best and Worst Calibration Hydrographs Based on Volume

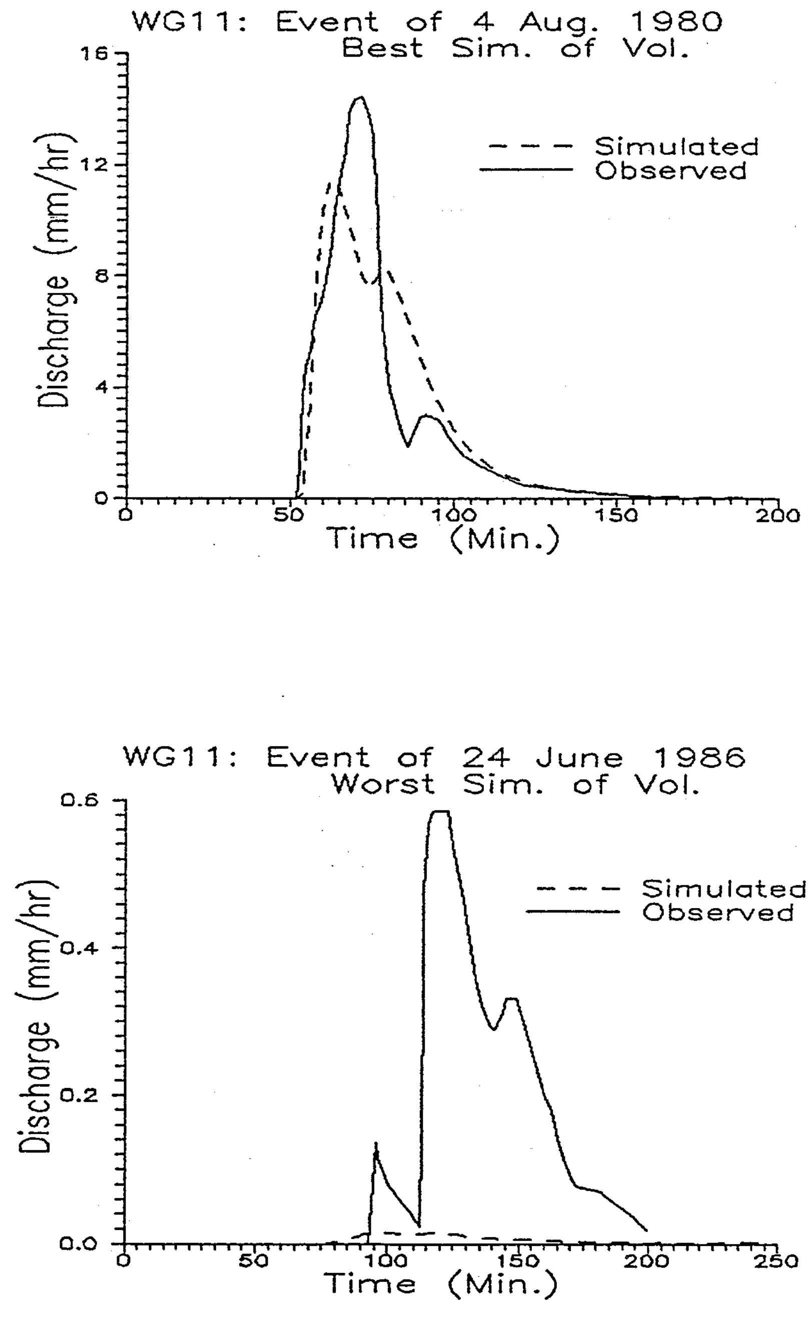

Figure 5.16 WG11: Best and Worst Calibration Hydrographs Based on Volume

multipliers obtained for the individual internal watersheds. An overall assessment of internal model accuracy is obtained by recomputing E_f for LH-106 and LH-102 when the parameter multipliers for LH-104 are used in the internal catchment simulations. For LH-106, using LH-104 multipliers, the calibration forecast efficiency (E_f) is 0.91 and 0.86 for runoff volume and peak rate, respectively. Comparable efficiencies for LH-102 are 0.96 and 0.97. Therefore, using the LH-104 multipliers caused virtually no change in the LH-102 efficiencies and about a ten percent decrease in the efficiencies for LH-106 (see Table 5.4). The coefficient of efficiency is influenced to a greater extent by the larger events in the set of interest. The good efficiencies obtained by using LH-104 multipliers for the internal basin suggest a good deal of internal model accuracy for medium to large events.

5.4 Conclusions

Sensitivity analysis was carried out on the smallest watershed analyzed (LH-106) to identify parameters to be used in model calibration. Parsimony of parameters was obtained by using parameter multipliers which scale, distributed, field estimated parameters linearly. The sensitivity analysis justified the selection of three overall watershed parameter multipliers. The three multipliers were M_K, M_C, and M_R, which are applied to the distributed model parameters Ks, C_v, and R1 (roughness), respectively.

Model performance was measured primarily by the coefficient of efficiency (E: Nash and Sutcliffe, 1970) for runoff volume and secondarily for peak runoff rate.

Technical Report No. HWR 91-010 June 1990

BASIN SCALE AND RUNOFF MODEL COMPLEXITY

by

David Charles Goodrich

Adjunct Assistant Professor

Department of Hydrology and Water Resources

University of Arizona

Tucson, Arizona, 85721

and

Research Hydraulic Engineer

USDA - Agricultural Research Service

Southwest Watershed Research Center

Tucson, Arizona 85719

Technical Reports on
Natural Resource Systems

APPENDIX 2

"Apparent Abstraction Rates in Ephemeral Stream Channels"

Volume 17

HYDROLOGY and WATER RESOURCES in ARIZONA and the SOUTHWEST

PROCEEDINGS OF THE 1987 MEETINGS
OF THE
ARIZONA SECTION --
AMERICAN WATER RESOURCES ASSOCIATION,
HYDROLOGY SECTION --
ARIZONA-NEVADA ACADEMY OF SCIENCE
AND THE
ARIZONA HYDROLOGICAL SOCIETY

APRIL 18, 1987, NORTHERN ARIZONA UNIVERSITY
FLAGSTAFF, ARIZONA

APPARENT ABSTRACTION RATES IN EPHEMERAL STREAM CHANNELS

Carl Unkrich and Herbert B. Osborn

USDA-ARS Aridland Watershed Management Research Unit, 2000 E. Allen Rd., Tucson, Arizona 85719.

INTRODUCTION

Modeling flow in a broad, sandy ephemeral stream channel is complicated by the presence of transient, meandering subchannels. These erosive features affect the hydraulic properties of the channel as well as the area available for infiltration into the bed. Models which simulate erodable channels are complex, require extensive data, and are not well verified (Dawdy and Vanoni, 1986, Chang, 1984). Models which simulate stable channels, however, are widely used by scientists and engineers. The purpose of this study was to evaluate the performance of a well-tested, stable channel model when used to simulate flow in an erodable channel.

STUDY REACH

The study area is located within the Walnut Gulch Experimental Watershed near Tombstone, Arizona, and is operated by the Agricultural Research Service of the USDA. The main channel is 2.6 miles long and from 40 to 100 feet wide, with a deep sand bed and stable banks. There are four main tributaries, all equipped with flumes to measure flow into the main channel.

PREVIOUS STUDIES

There have been several studies of runoff in the ephemeral stream channels on Walnut Gulch. Keppel and Renard (1962) reported that transmission losses are influenced by antecedent moisture conditions within the channel alluvium, peak discharge at the upstream gaging station, duration of flow, channel width, and quantity and texture of the channel alluvium. They found abstraction rates ranging from 0.2 to 9 ac-ft/mi/hr in the lower reaches of Walnut Gulch. Renard and Keppel (1966) then reported on the influence of translation waves and transmission losses on the shape of the runoff hydrograph. Renard and Laursen (1975) explained the cancellation of greater downstream transmission losses by tributary inflow. Freyburg (1983) stated that, for ephemeral streams, the infiltration along the channel is a complex function of bed material, channel geometry, and hydrograph shape. Smith (1972) described the kinematic modeling of shock-type flood waves and recognized its potential as a tool for studying transmission losses in ephemeral streams.

MODEL DESCRIPTION

The model employed a four point implicit finite difference method for estimating the solution of the combined continuity and uniform flow equations ("kinematic wave") for flow area in channel segments with uniform slopes and trapezoidal cross sections (Rovey, Woolhiser and Smith, 1977). The routing equations included a transmission loss component, which for this study was approximated by a constant abstraction rate.

PROCEDURE

(1) The study reach was discretized into segments; each segment was assigned uniform properties (Fig. 1, Table 1).

(2) Seven flood events, for which intermediate inflow along the study reach could be neglected, were identified. They included two events originating from flume 8; two from flumes 9 and 15 combined; one from flumes 8,9,10 and 15; one from flumes 8,9 and 10; and one from flumes 9 and 10.

(3) Simulated hydrographs were adjusted to match the observed hydrographs by selecting an optimal bed abstraction rate for each event.

RESULTS

The optimal simulations required a range of abstraction rates from 1.0 to 6.5 iph, or 0.67 to 4.36 ac-ft/mi/hr, a subset of the range found by Keppel and Renard. The resulting simulated peak flows and flow volumes were mostly very close to the observed values (Figs. 4-9). Bed abstraction rates were plotted against corresponding values of both peak discharge and inflow volume (Figs. 2 and 3). The plots suggest a relationship between abstraction rate and the magnitude of the event.

CONCLUSIONS

There is no theoretical justification for assigning a different abstraction rate to each event, unless the range of abstraction rates can be explained by antecedent moisture conditions alone; inspection of flow records indicated this was not the case. Therefore, most of the difference must be attributed to the initial configuration of the channel and its evolution during the event, i.e., the formation of subchannels. Although our model cannot simulate these subchannels directly, it may be possible to model their effect by abandoning the explicit geometrical representation and making the area-discharge curve a function of some aspect of the flow. By constructing different area-discharge curves, the kinematic model could be used to quickly test assumptions about the relationship between channel flow, morphology, and abstraction. Until this is done, the use of a stable channel model to route flow in broad, sandy ephemeral stream channels cannot be recommended.

References Cited

Chang, H. H. 1984. Modeling of River Channel Changes. Journal of Hydraulic Engineering, ASCE, 110(2):157-172.

Dawdy, D. R. and V. A. Vanoni. 1986. Modeling Alluvial Channels. Water Resources Research, AGU, 22(9):71-81.

Freyburg, D. L. 1983. Modeling the Effects of a Time-Dependent Wetted Perimeter on Infiltration From Ephemeral Channels. Water Resources Research, AGU, 19(2):559-566.

Keppel, R. V. and K. G. Renard. 1962. Transmission Losses in Ephemeral Stream Beds. Journal of the Hydraulics Division, ASCE, 88(HY3):59-68.

Renard, K. G. and R. V. Keppel. 1966. Hydrographs of Ephemeral Streams in the Southwest. Journal of the Hydraulics Division, ASCE, 92(HY2):33-52.

Renard, K. G. and E. M. Laursen. 1975. A Dynamic Behavior Model of an Ephemeral Stream. Journal of the Hydraulics Division, ASCE, 101(HY5):511-528.

Rovey, E. W., Woolhiser, D. A. and R. E. Smith. 1977. A Distributed Kinematic Model of Upland Watersheds. Hydrology Paper No. 93, Colorado State University, 52 p.

Smith, R. E. 1972. Border Irrigation Advance and Ephemeral Flood Waves. Journal of the Irrigation and Drainage Division, ASCE, 98(IR2):289-307.

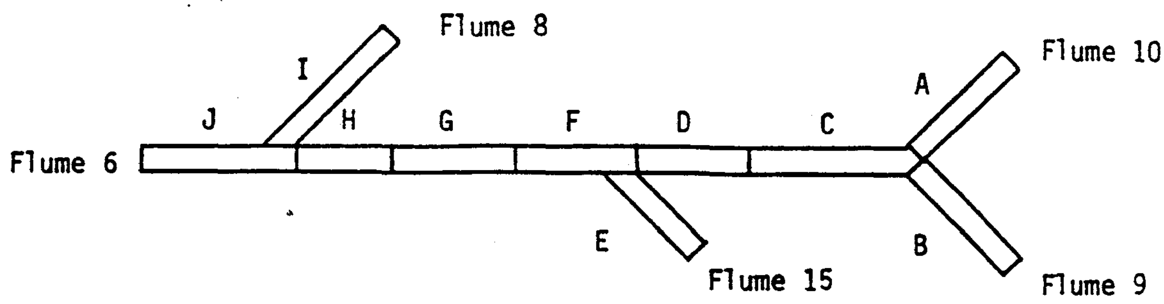

Figure 1. Schematic of Model Representation.

Table 1. Properties of Channel Segments.

Segment	Length (ft)	Width (ft)	Slope
A	524	30	.0113
B	271	20	.0113
C	4617	40	.0113
D	1707	65	.0099
E	339	20	.0090
F	2527	65	.0151
G	1988	40	.0105
H	1331	100	.0117
I	2722	45	.0136
J	1675	100	.0112

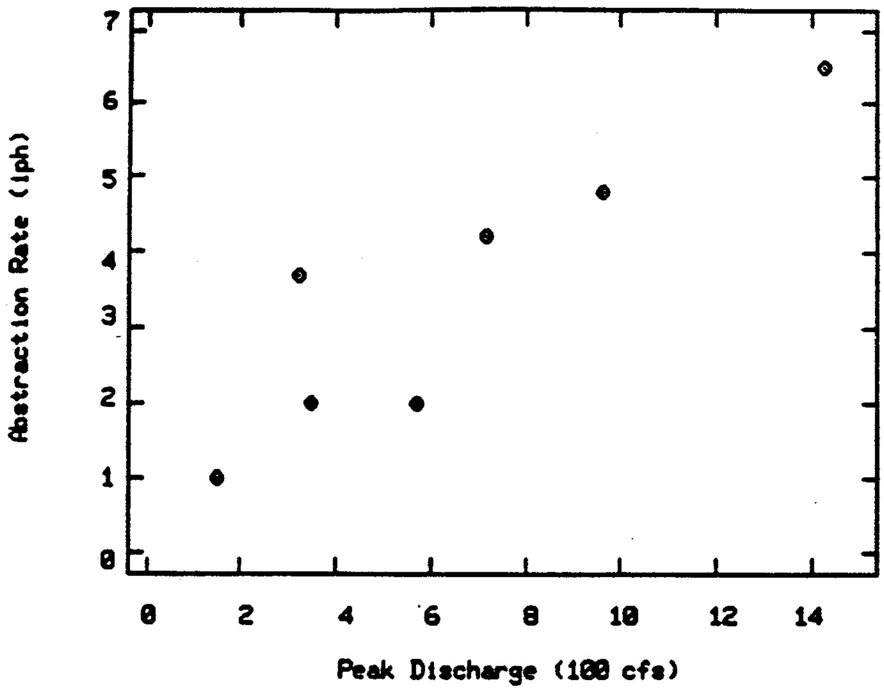

Figure 2. Abstraction versus peak discharge.

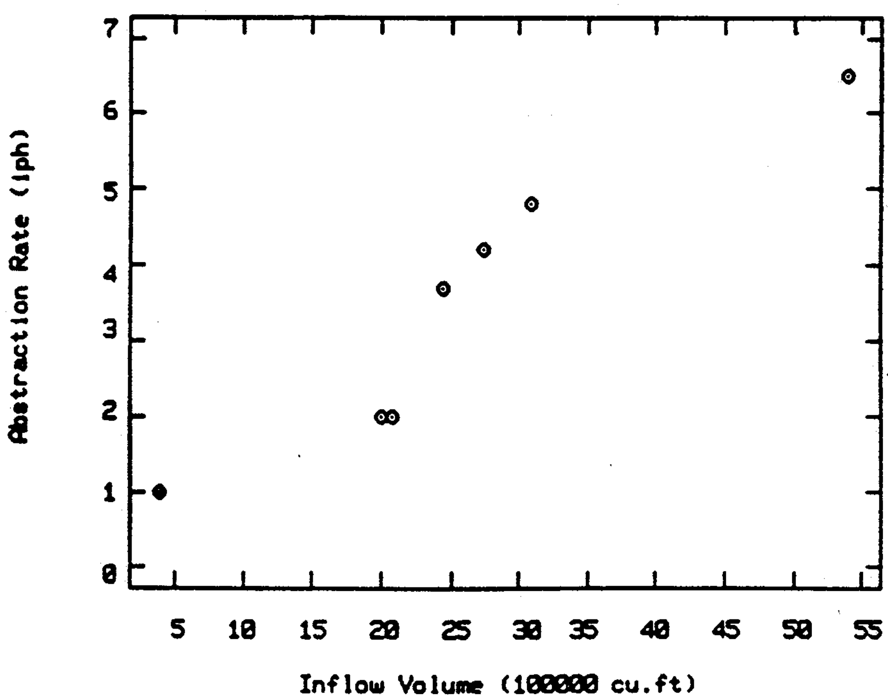

Figure 3. Abstraction versus inflow volume.

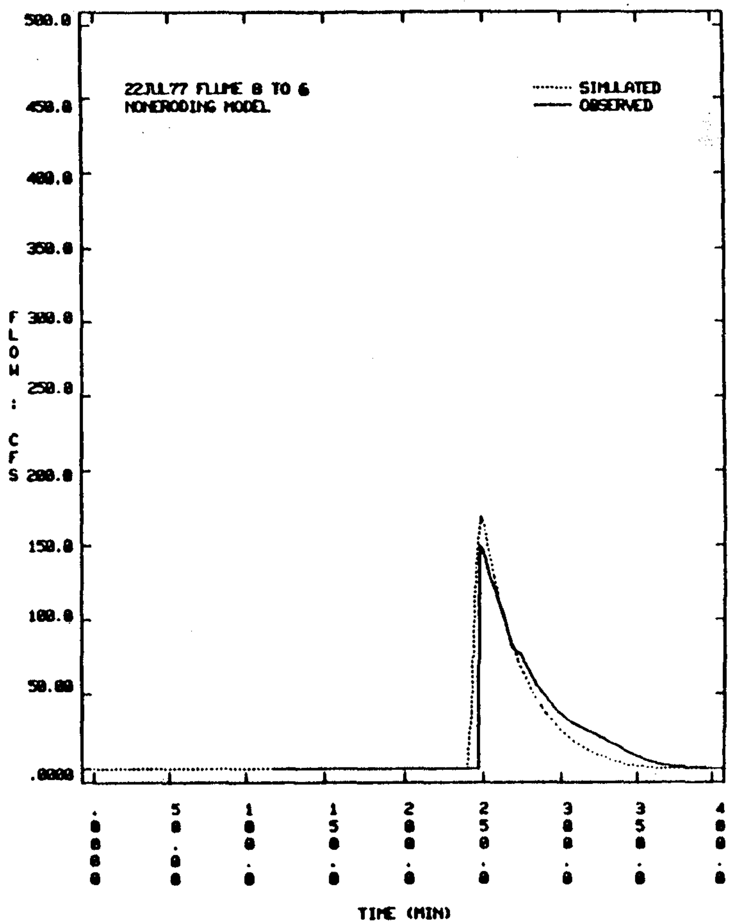

Figure 4. Event with 1.0 iph abstraction.

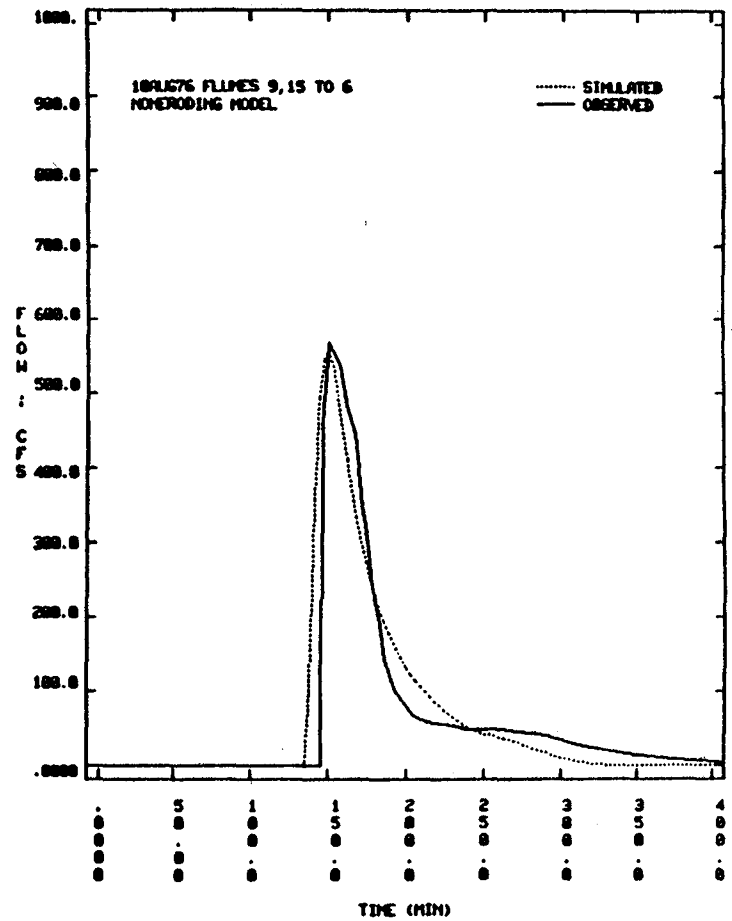

Figure 5. Event with 2.0 iph abstraction.

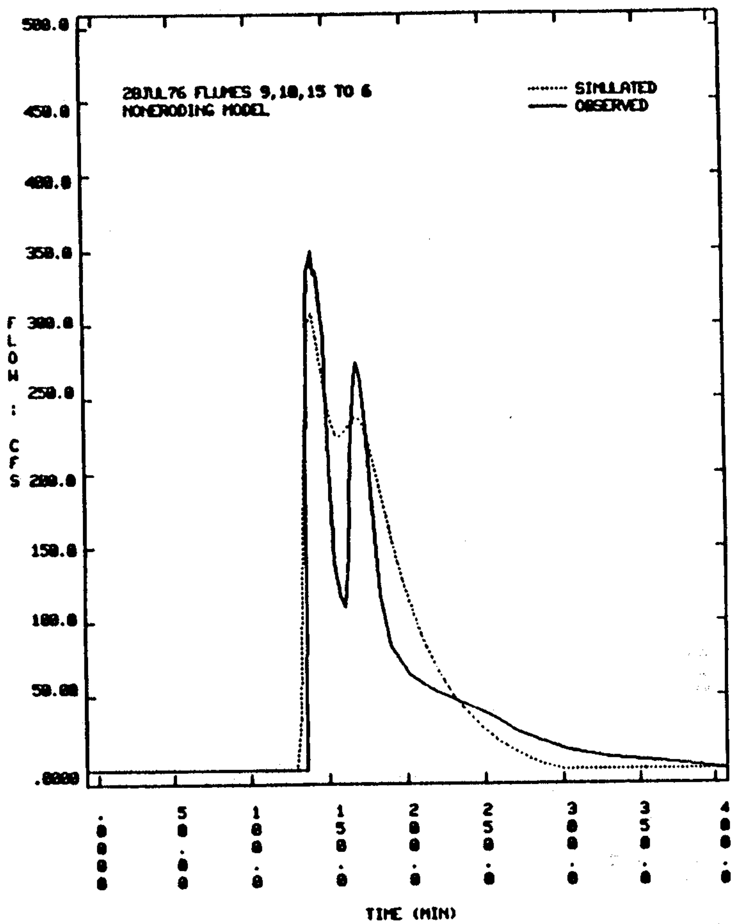

Figure 6. Event with 2.0 iph abstraction.

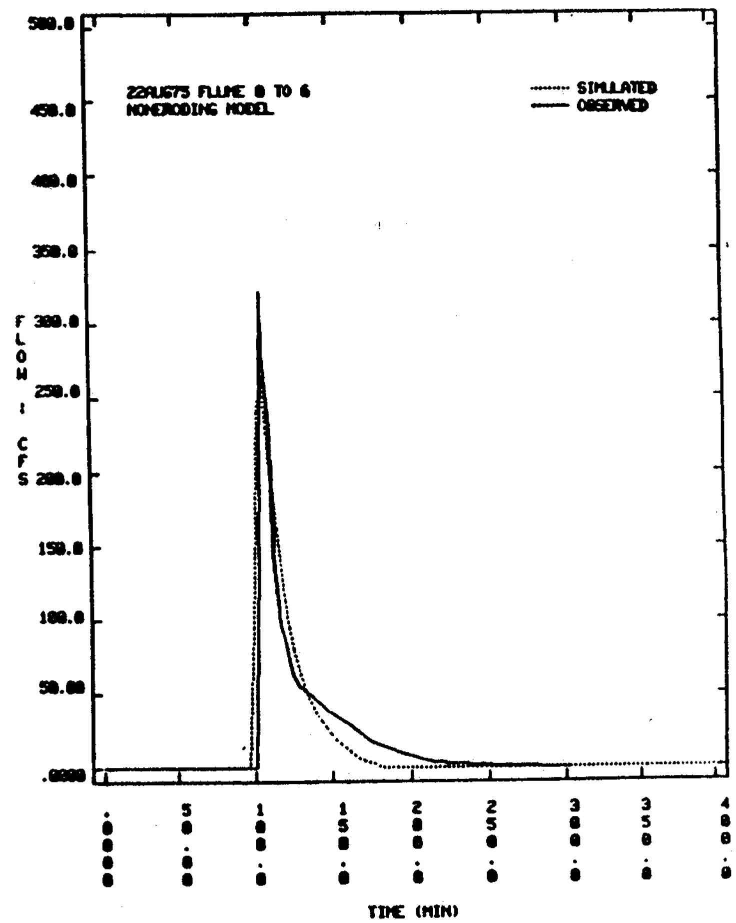

Figure 7. Event with 3.7 iph abstraction.

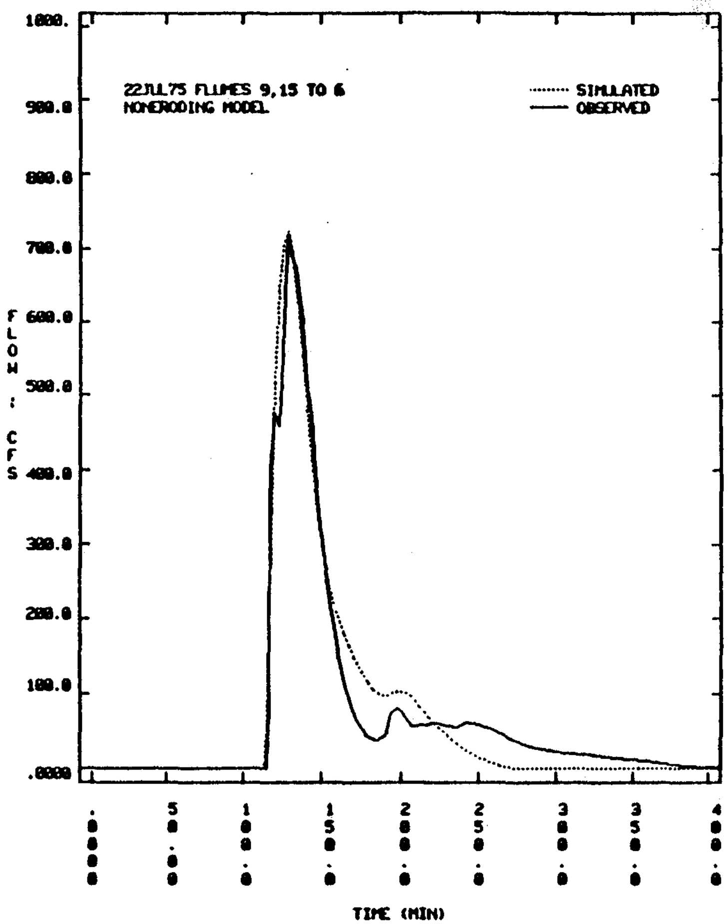

Figure 8. Event with 4.2 iph abstraction.

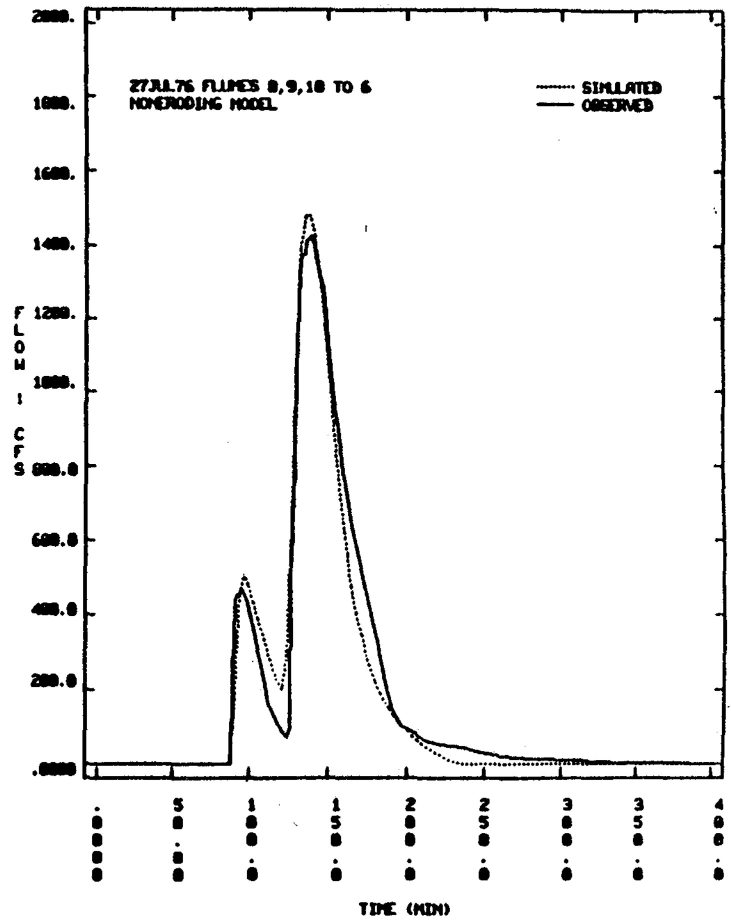

Figure 9. Event with 6.5 iph abstraction.

APPENDIX 3

Channel Loss Information

Walnut Gulch - Total Rainfall Depth for 18 Aug 74 Event Showing Flume Locations and Boundaries for Subwatersheds 6, 8, 9, 10, 15

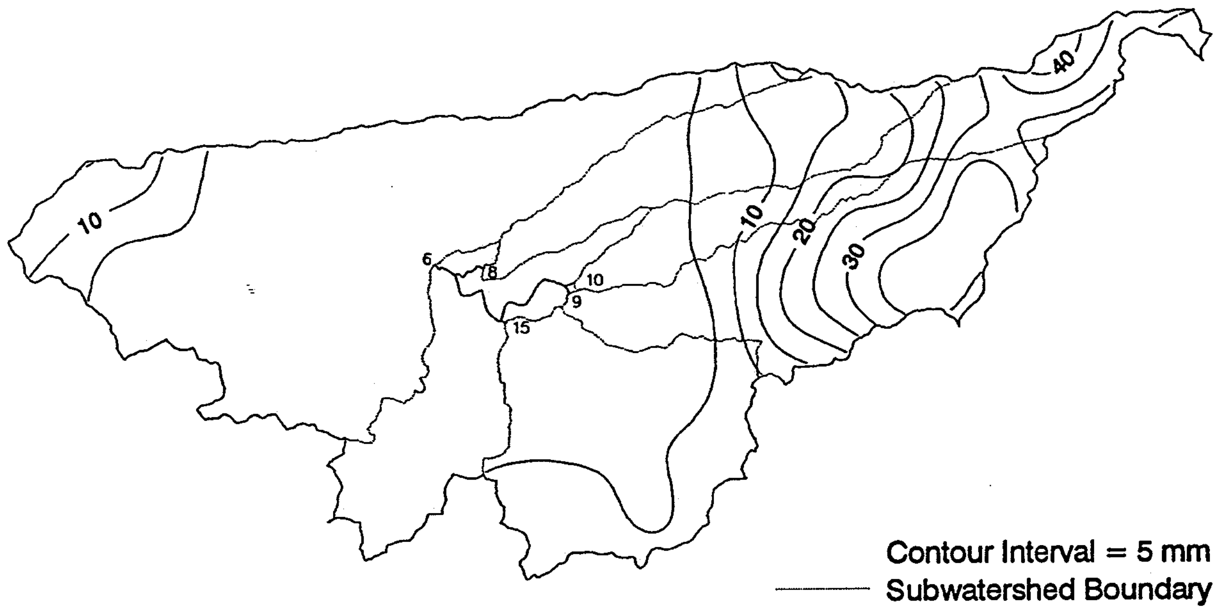

Walnut Gulch - Total Rainfall Depth for 22 Jul 75 Event Showing Flume Locations and Boundaries for Subwatersheds 6, 8, 9, 10, 15

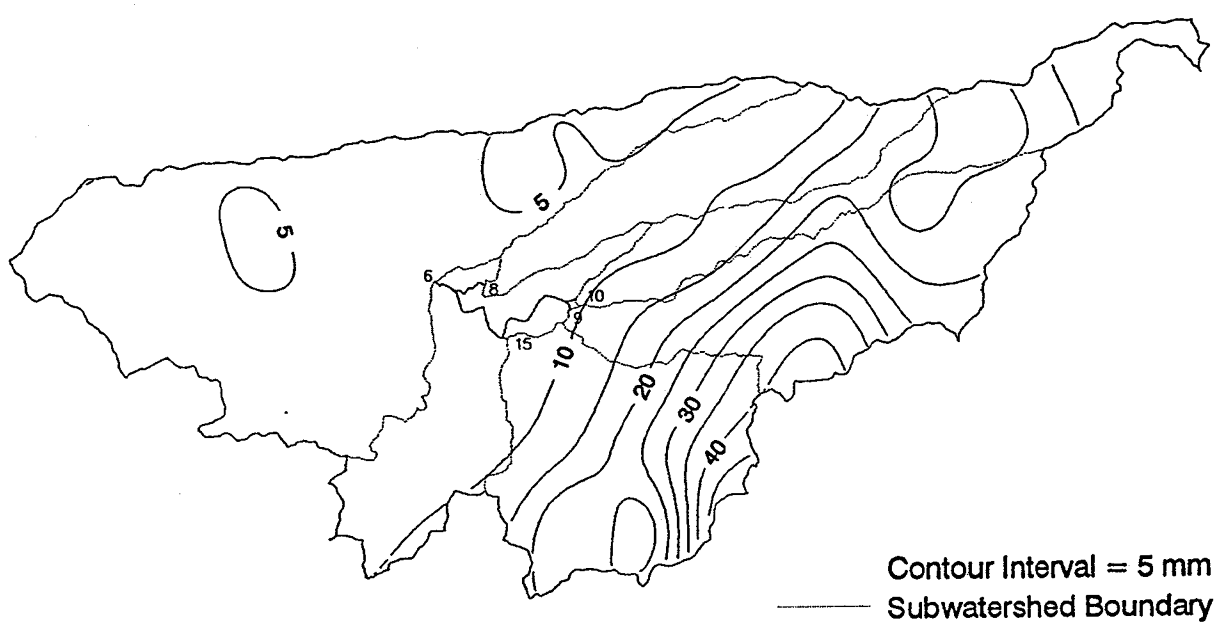

Walnut Gulch - Total Rainfall Depth for 22 Aug 75 Event Showing Flume Locations and Boundaries for Subwatersheds 6, 8, 9, 10, 15

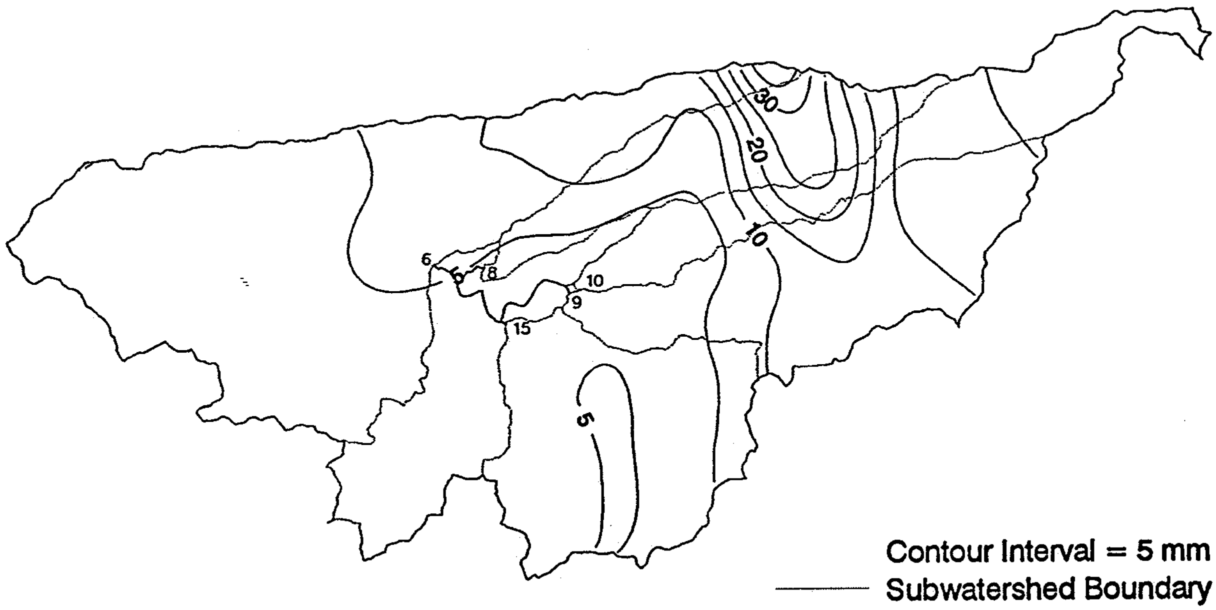

Walnut Gulch - Total Rainfall Depth for 28 Jul 76 Event Showing Flume Locations and Boundaries for Subwatersheds 6, 8, 9, 10, 15

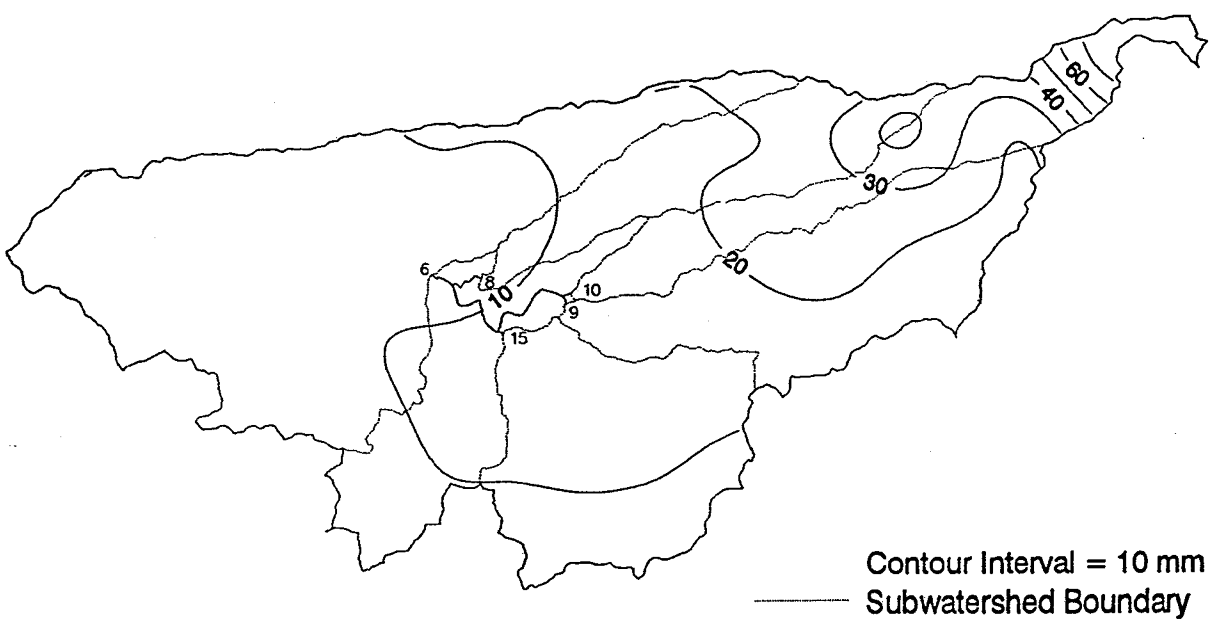

Walnut Gulch - Total Rainfall Depth for 10 Aug 76 Event Showing Flume Locations and Boundaries for Subwatersheds 6, 8, 9, 10, 15

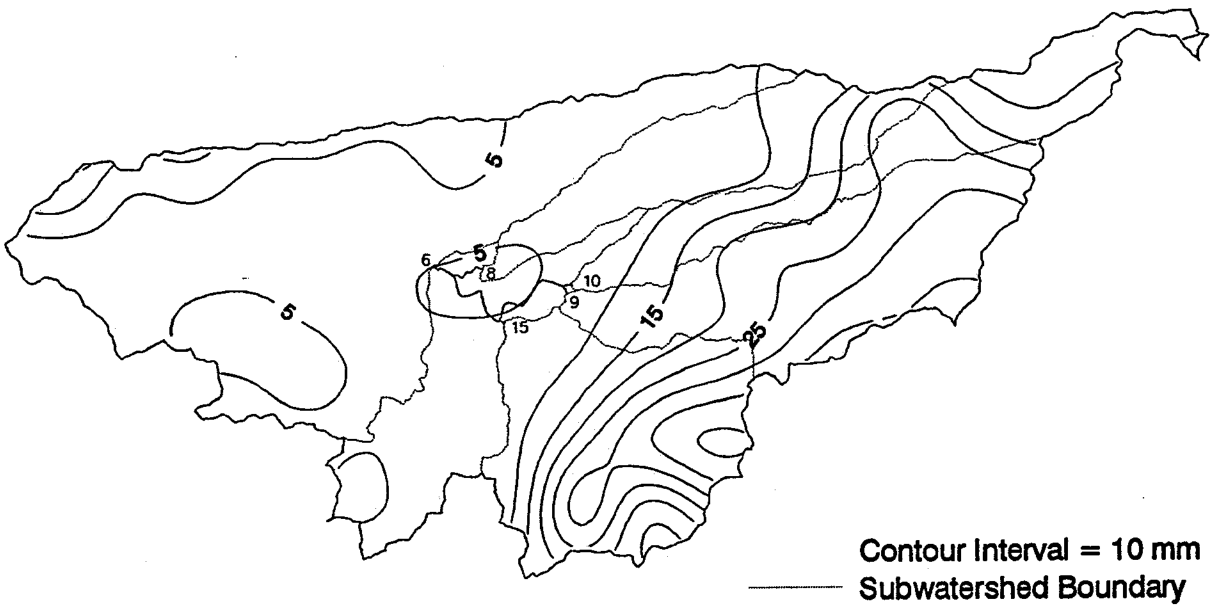

Description of Channel Reach Used for Routing Test

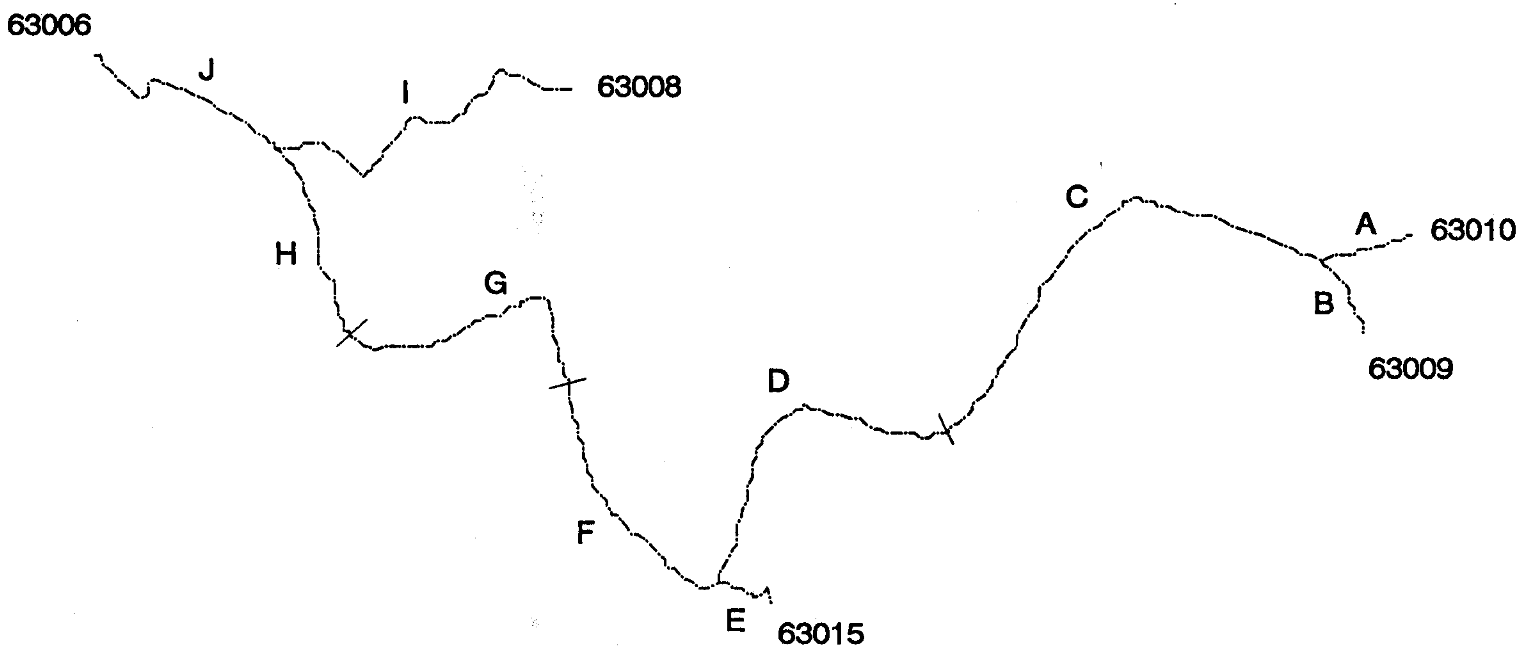

SEGMENT	LENGTH (ft)	WIDTH (ft)	SLOPE
A	738	30	.0113
B	643	20	.0113
C	4617	40	.0113
D	1707	65	.0099
E	430	20	.0090
F	2527	65	.0151
G	1988	40	.0105
H	1331	100	.0117
I	2722	45	.0136
J	1675	100	.0112

FOR ALL SEGMENTS

Cross section bank slopes: 1:1
Manning n: 0.02
Saturated hydraulic conductivity: 8.3 iph
Capillary suction: 1.8 in.

Infiltration parameters were estimated based on textural class from Rawls, W.J., D.L. Brakensiek, and K.E. Saxton "Estimation of Soil Water Properties" in Transactions of the ASCE 25(5):1316-1320,1328 (1982)

Schematic Cross Section Defining Effective Wetted Perimeter Calculation in KINEROS

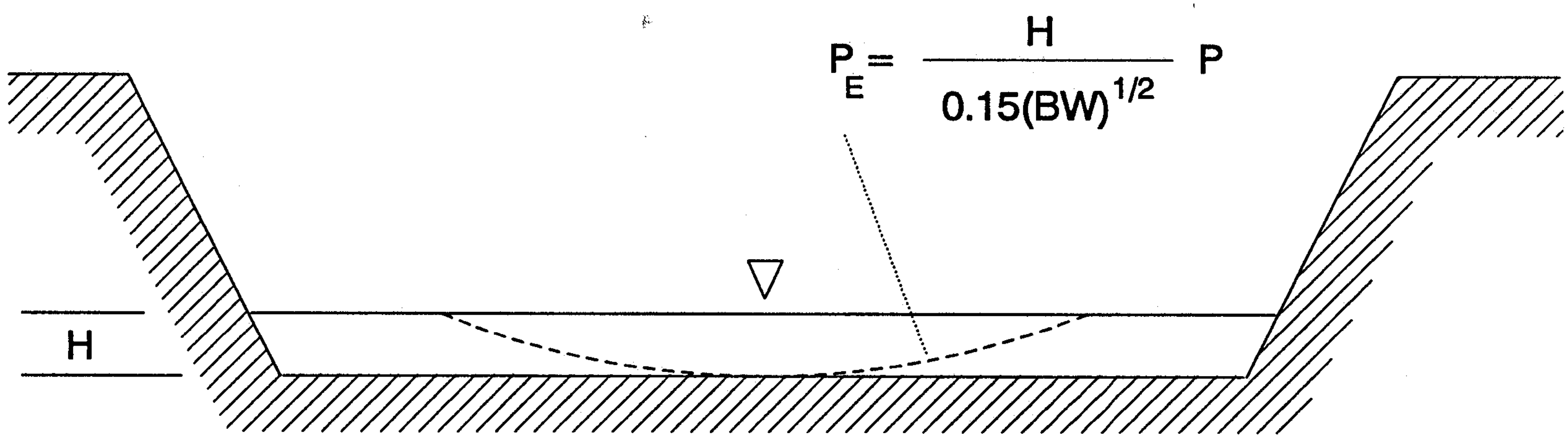

Vertical Scale Exagerated

P = wetted perimeter of trapezoidal section at depth H

P_E = effective wetted perimeter until $H = 0.15(BW)^{1/2}$

BW = bottom width of trapezoidal section